

1 **Short title: *AtMOB1s* regulate jasmonate and development**

2

3 Corresponding author:

4 Youfa Cheng,

5 Key Laboratory of Plant Molecular Physiology, Institute of Botany, Chinese Academy

6 of Sciences, Beijing 100093, China.

7 University of Chinese Academy of Sciences, Beijing 100049, China.

8 Tel: +86 10 6283 6882

9 Email: [yfcheng@ibcas.ac.cn](mailto:yfcheng@ibcas.ac.cn)

10

11 **Title: *AtMOB1* genes regulate jasmonate accumulation and plant development**

12

13 Zhiai Guo<sup>1</sup>, Xiaozhen Yue<sup>1,2</sup>, Xiaona Cui<sup>1,2</sup>, Lizhen Song<sup>1</sup>, Youfa Cheng<sup>1,2</sup>

14

15 1. Key Laboratory of Plant Molecular Physiology, Institute of Botany, Chinese

16 Academy of Sciences, Beijing 100093, China.

17 2. University of Chinese Academy of Sciences, Beijing 100049, China.

18

19 **One-sentence summary**

20 A core component of the Hippo pathway plays important roles in regulating jasmonate

21 accumulation and plant development in Arabidopsis.

22

23 **Author contributions**

24 Y.C. conceived and designed research; Z.G., X.Y., X.C., and L.S. performed the

25 experiments; Z.G. and Y.C. analyzed data; Z.G. and Y.C. wrote the paper.

---

26

27 **Funding:**

28 This work was supported by the projects from the National Natural Science Fund of  
29 China (31970309; 31171389; 91217310; 91017008; 31270330), National Key  
30 Research and Development Program of China (2016YFD0100400), National Basic  
31 Research Program of China (2014CB943400), and One-hundred Talent Project of the  
32 Chinese Academy of Sciences to YC.

33

34 **Corresponding author email:** [yfcheng@ibcas.ac.cn](mailto:yfcheng@ibcas.ac.cn)

35

36

---

37 **Abstract**

38

39 The MOB1 proteins are highly conserved in yeasts, animals, and plants.  
40 Previously, we showed that the Arabidopsis *MOB1A* gene (*AtMOB1A/NCP1*) plays  
41 critical roles in auxin-mediated plant development. Here, we report that *AtMOB1A*  
42 and *AtMOB1B* redundantly and negatively regulate jasmonate (JA) accumulation and  
43 function in Arabidopsis development. The two *MOB1* genes exhibited similar  
44 expression patterns and the MOB1 proteins displayed similar subcellular localizations  
45 and physically interacted in vivo. Furthermore, the *atmob1a atmob1b (mob1a/1b)*  
46 double mutant displayed severe developmental defects, which were much stronger  
47 than those of either single mutant. Interestingly, many jasmonate-related genes were  
48 up-regulated in *mob1a/1b*, suggesting that AtMOB1A and AtMOB1B negatively  
49 regulate the JA pathways. *mob1a/1b* plants accumulated more JA and were  
50 hypersensitive to exogenous JA treatments. Disruption of *MYC2*, a key gene in JA  
51 signaling, in the *mob1a/1b* background partially alleviated the root defects and JA  
52 hypersensitivity observed in *mob1a/1b*. Moreover, the expression levels of the  
53 *MYC2*-repressed genes *PLT1* and *PLT2* were significantly decreased in the *mob1a/1b*  
54 double mutant. Our results showed that *MOB1A/1B* genetically interact with *SIK1* and  
55 antagonistically modulate JA-related gene expression. Taken together, our findings  
56 indicate that AtMOB1A and AtMOB1B play important roles in regulating JA  
57 accumulation and Arabidopsis development.

58

59 **Key words:** Hippo pathway, *MOB1A*, *MOB1B*, *SIK1*, jasmonate, Arabidopsis, root,  
60 development

61

62 **Introduction**

63

64 The Hippo signaling pathway was first described in animals. It plays pivotal roles  
65 in controlling cell proliferation, apoptosis, organ growth, and tissue homeostasis (Pan,  
66 2010). Dysregulation of the pathway causes various cancers (Harvey et al., 2013). The

---

67 core components of the pathway, including the Ste20-like kinases MST1/2, the AGC  
68 kinase NDR/LATS, and the kinase regulators MOB1 and Sav, form a kinase cascade.  
69 Sav interacts with MST1/2 and activates its kinase activity. MST1/2 phosphorylates  
70 NDR/LATS kinase and MOB1. Subsequently, MOB1 interacts with NDR/LATS and  
71 regulates kinase activity of the latter. The activated NDR/LATS in turn phosphorylates  
72 and inactivates the transcriptional co-activator YAP/TAZ (Hansen et al., 2015).

73

74 The MOB1 proteins are highly conserved from yeast (*Saccharomyces cerevisiae*)  
75 to plants and animals (Lai et al., 2005; Cui et al., 2016). The yeast *MOB1* is an  
76 essential gene required for completion of mitosis and maintenance of ploidy (Luca  
77 and Winey, 1998). In *Drosophila* (*Drosophila melanogaster*), disruption of  
78 *MOB1/Mats* results in increased cell proliferation, defective apoptosis, and induction  
79 of tissue overgrowth (Lai et al., 2005). In humans (*Homo sapiens*), among the 7  
80 homologs of yeast MOB (hMOB1A, 1B, 2A, 2B, 2C, 3, 4), hMOB1A and hMOB1B  
81 share more than 95% sequence identity/similarity. A biochemical characterization of  
82 hMOBs showed that only hMOB1A and hMOB1B interact with both LATS1 and  
83 LATS2 to regulate cell proliferation and apoptosis (Chow et al., 2010). In mouse  
84 (*Mus musculus*), the *mob1a/1b* double mutant showed cancer susceptibility and  
85 embryonic lethality (Nishio et al., 2012). *Mob1a/1b* double mutation in mouse liver  
86 results in the death of more than half of mutant mice within 3 weeks of birth. All  
87 survivors eventually develop liver cancers and die by age 60 weeks (Nishio et al.,  
88 2016). In addition, tamoxifen-inducible, chondrocyte-specific *Mob1a/b*-deficient mice  
89 had chondrodysplasia (Goto et al., 2018).

90

91 The Arabidopsis genome contains four *MOB1* genes: *AtMOB1A*, *AtMOB1B*,  
92 *AtMOB1C*, and *AtMOB1D* (Citterio et al., 2006; Vitulo et al., 2007; Cui et al., 2016).  
93 *AtMOB1A* is required for tissue patterning of the root tip, and sporophyte and  
94 gametophyte development (Galla et al., 2011; Pinosa et al., 2013). Recently, we  
95 reported that *AtMOB1A* plays critical roles in auxin-mediated plant development (Cui  
96 et al., 2016). The *atmob1a* mutant genetically interacts with mutants in auxin

---

97 biosynthesis, signaling, and transport in many developmental processes. Interestingly,  
98 the defects of *atmob1a* can be fully rescued by the *Drosophila MOB1* gene *Mats*,  
99 suggesting conserved gene functions among different species (Cui et al., 2016). It was  
100 shown that AtMOB1A and AtMOB1B interact with SIK1, a Hippo/STE20 homolog,  
101 and regulate cell proliferation and expansion in Arabidopsis (Xiong et al., 2016). These  
102 findings demonstrate that AtMOB1A plays important roles in plant development.  
103 However, the functions of other Arabidopsis *MOB1* genes remain to be elucidated.

104

105 Jasmonates (JAs) are a group of phytohormones including jasmonic acid and its  
106 derivatives. They are important in regulating plant growth and development, and plant  
107 responses to biotic and abiotic stresses. Jasmonic acid is synthesized from  $\alpha$ -linolenic  
108 acid via the octadecanoid pathway in plastids and peroxisomes. Following synthesis,  
109 jasmonic acid is exported from the peroxisomes into the cytoplasm, where it is  
110 conjugated with isoleucine to produce bioactive JA-Ile. In the JA signaling pathway,  
111 JA-Ile promotes the interaction between the JA receptor COI1 and JAZ proteins. JAZ  
112 can be ubiquitinated and degraded by the 26S proteasome, leading to the release of  
113 MYC2, the major transcription factor of jasmonate-mediated gene expression.  
114 Consequently, the JA responsive gene expression and JA responses are activated  
115 (Huang et al., 2017).

116

117 Here we show that the *mob1a/1b* double mutant displays severe developmental  
118 defects at the seedling stage. *AtMOB1B* expression was similar to that of *AtMOB1A*,  
119 and the two MOB1 proteins interacted with each other in vivo. Transcriptomic  
120 analysis indicated that the expression levels of many genes in the JA pathways were  
121 increased in the *mob1a/1b* double mutant. JA contents were also significantly  
122 increased in *mob1a/1b*. Consistently, *mob1a/1b* displayed hypersensitivity to  
123 exogenous JA treatments and the expression of *MYC2*, which encodes a key  
124 transcription factor in JA signaling, was increased. Moreover, *myc2* partially  
125 suppressed the developmental defects of *mob1a/1b*. We found that the expression  
126 levels of MYC2-repressed *PLT1* and *PLT2* in the *mob1a/1b* double mutant were

---

127 significantly decreased. We conclude that AtMOB1A and AtMOB1B regulate JA  
128 accumulation, and plant growth and development.

129

## 130 **Results**

131

### 132 ***AtMOB1A* and *AtMOB1B* redundantly control plant development**

133 There are four *MOB1* genes in Arabidopsis, namely *AtMOB1A*, *AtMOB1B*,  
134 *AtMOB1C*, and *AtMOB1D* (Citterio et al., 2006; Vitulo et al., 2007; Cui et al., 2016).  
135 *AtMOB1A* and *AtMOB1B* form a subgroup, whereas *AtMOB1C* and *AtMOB1D* form  
136 another clade (Fig. 1A). Previously, we reported that the loss-of-function *MOB1A*  
137 mutants, *mob1a-1* and *mob1a-2*, developed short roots and displayed small floral  
138 organs and reduced fertility compared to wild type (WT) (Cui et al., 2016).

139 To define functions of the other *AtMOB1* genes, we obtained T-DNA insertion  
140 mutants, denoted *mob1b-1*, *mob1c-1*, and *mob1d-1* (Fig. 1B), from the Nottingham  
141 Arabidopsis Stock Center. RT-PCR analysis indicated that all of the mutations  
142 appeared null (Fig. S1A). However, no obvious developmental defects were observed  
143 in the single mutants, suggesting that the *MOB1* genes may have overlapping  
144 functions. We then generated the double and triple mutant combinations (Fig. 1C-J).  
145 Because *MOB1C* (*At5g20430*) and *MOB1D* (*At5g20440*) are located in tandem on  
146 Chromosome V, it is impossible to generate the double mutant or the quadruple  
147 mutant by genetic crossing. We thus constructed the *mob1a-2 mob1b-1 mob1c-2*  
148 *mob1d-1* quadruple mutant (*mob1a-2/b-1/c-2/d-1*) using CRISPR/Cas9 gene editing  
149 technology (Gao et al., 2016) (Zeng et al., 2018) (Fig. 1K, and Fig. S1B) in the  
150 *mob1a-2<sup>+/-</sup>/mob1b-1/mob1d-1* (*mob1a-2<sup>+/-</sup>/b-1/d-1*) background.

151 The seedlings of *mob1a-2/b-1<sup>+/-</sup>* displayed smaller cotyledons, shorter roots,  
152 and a longer hypocotyl than single mutants and WT (Fig. 1D-E). The siliques of  
153 *mob1a-2/b-1<sup>+/-</sup>* adult plants were very short and completely sterile (Fig. 1F-G). On the  
154 other hand, the *mob1a-2<sup>+/-</sup>/b-1* mutant resembled *mob1b-1*. These results indicated  
155 that *AtMOB1B* became haploid insufficient in the *mob1a* mutant background. The  
156 *mob1a-2/b-1* seedlings were very tiny, and their development was significantly

---

157 retarded. The 21-d-old double-mutant plants had much smaller leaves and shorter  
158 roots compared to WT and the single mutants (Fig. S2). To confirm that the  
159 phenotypes were caused by the mutations in *AtMOB1A* and *AtMOB1B*, we carried out  
160 genetic complementation experiments. Transformation of *mob1a-2/b-1* with the  
161 *AtMOB1A* genomic fragment resulted in plants that were similar to *mob1b-1*. We also  
162 found that *mob1a-2/b-1* plants harboring the *AtMOB1B* transgene behaved similarly  
163 to *mob1a*. Our results demonstrate that the strong developmental defects observed in  
164 the *mob1a-2/b-1* mutant are caused by the disruption of both *AtMOB1A* and  
165 *AtMOB1B* (Fig. S3).

166 The *mob1a-1/b-1/c-1* and *mob1a-2/b-1/d-1* triple mutants and the  
167 *mob1a-2/b-1/c-2/d-1* quadruple mutant displayed phenotypes similar to that of  
168 *mob1a-2/b-1* (Fig. 1H-J). Moreover, the *mob1c-2/d-1* double mutant segregated from  
169 the *mob1a-2/b-1/c-2/d-1* quadruple mutant similar to the *mob1c-1* and *mob1d-1*  
170 single mutants and WT plants (Fig. 1L). These results suggest that *AtMOB1A* plays a  
171 more predominant role than *AtMOB1B*. *AtMOB1A* and *AtMOB1B* appear to be more  
172 important in regulating plant development than *AtMOB1C* and *AtMOB1D* under our  
173 growth conditions. We therefore focused on *AtMOB1A* and *AtMOB1B* in this work.

174

### 175 ***AtMOB1A* and *AtMOB1B* show similar expression patterns**

176 To investigate the expression patterns of *AtMOB1A* and *AtMOB1B*, we made  
177 constructs containing *AtMOB1A* or *AtMOB1B* genomic DNA sequences fused with  
178 the *GUS* gene, which were then expressed in WT plants. *AtMOB1A-GUS* and  
179 *AtMOB1B-GUS* were expressed with very similar patterns in cotyledons, true leaves,  
180 trichomes, root hairs, primary and lateral roots of seedlings, and floral organs (Fig.  
181 S4A-F, and H-M).

182 We also generated transgenic plants containing *AtMOB1B* genomic DNA  
183 sequence fused with the *GFP* gene. *AtMOB1B-GFP* was expressed in the roots, and  
184 the fusion protein was localized to the nucleus, cytoplasm, and plasma membrane,  
185 similar to *AtMOB1A-GFP* (Fig. S4G and N). The subcellular localization of  
186 *AtMOB1B-GFP* was similar to that of *AtMOB1A-GFP* (Cui et al., 2016). These

---

187 results are consistent with our hypothesis that *AtMOB1A* and *AtMOB1B* redundantly  
188 regulate plant development.

189

### 190 ***AtMOB1A* and *AtMOB1B* are necessary for cell proliferation**

191 The seedlings of the *mob1a-2/b-1* mutant had very short roots. The lengths of the  
192 root elongation zone and the meristem zone were dramatically decreased in the  
193 *mob1a-2/b-1* mutant (Fig. 2A-C). The cell numbers of the elongation zone and the  
194 meristem zone were also significantly reduced in the double mutant (Fig. 2D-E).  
195 Moreover, the root cap columella of *mob1a-2/b-1* was much smaller (Fig. 2F-G).  
196 These results suggest that cell division activities are abnormal in *mob1a-2/b-1*. To test  
197 this hypothesis, we used *CYCB1;1:GUS*, which is a widely used marker for the G2/M  
198 phase of the cell cycle (Colon-Carmona et al., 1999). We introduced this marker into  
199 the *mob1a-2/b-1* double and single mutant backgrounds by genetic crossing. The  
200 expression of *CYCB1;1:GUS* was decreased significantly in *mob1a-2* and slightly in  
201 *mob1b-1* single mutants, and was barely detectable in the *mob1a-2/b-1* double mutant  
202 (Fig. 2H-I). These results suggest that both *MOB1A* and *MOB1B* are important for  
203 cell proliferation in Arabidopsis roots.

204

### 205 **AtMOB1A physically interacts with AtMOB1B**

206 We tested whether AtMOB1A and AtMOB1B physically interact with each other.  
207 We carried out a co-immunoprecipitation (Co-IP) assay in *Nicotiana benthamiana*  
208 leaves, which were co-transformed with YFP-tagged AtMOB1B and FLAG-tagged  
209 AtMOB1A. The proteins were immuno-precipitated using anti-GFP beads and  
210 detected with FLAG antibody. Our results clearly indicated that AtMOB1A and  
211 AtMOB1B physically interact in *N. benthamiana* leaves (Fig. 3A).

212 We also performed immuno-precipitation mass spectrometry (IP-MS)  
213 experiments using Arabidopsis seedlings transformed with *35S::AtMOB1A-FLAG*.  
214 Total protein was extracted from seedlings and immuno-precipitated with anti-FLAG  
215 antibody beads. The candidate interacting proteins were then identified by mass  
216 spectrometry. A total of 11 AtMOB1A/B peptide sequences were detected as

---

217 AtMOB1A-interacting proteins. Although nine of these were shared by AtMOB1A/B,  
218 the other two were AtMOB1B specific (Table S1), indicating that AtMOB1A and  
219 AtMOB1B interacted in the IP-MS assay in Arabidopsis.

220 To further confirm the interaction, we carried out the firefly luciferase  
221 complementation imaging (LCI) assay (Chen et al., 2008). The results indicated that  
222 AtMOB1A directly interacts with AtMOB1B in *N. benthamiana* leaves (Fig. 3B).  
223 Combined, these experiments show that AtMOB1A interacts with AtMOB1B in vivo.

224

### 225 ***AtMOB1A* and *AtMOB1B* negatively regulate the jasmonate pathways**

226 To identify differentially expressed genes (DEGs) between the *mob1a-2/b-1*  
227 mutant and WT, we performed RNA-sequencing (RNA-seq) analysis using 10-d-old  
228 seedlings of *mob1a-2/b-1* and Col-0, with three biological repeats included of each  
229 genotype. A total of 1202 DEGs were identified, including 725 up-regulated and 477  
230 down-regulated genes (Supplemental Table S2). Gene Ontology (GO) analysis  
231 revealed that many genes in the jasmonic acid (JA) biosynthetic, metabolic, and  
232 signaling pathways were significantly enriched (Fig. 4A). In addition, genes involved  
233 in several JA-related biological processes were also enriched, including glucosinolate  
234 biosynthetic and metabolic processes, and responses to insects and wounding (Huang  
235 et al., 2017; Wasternack and Song, 2017) (Fig. 4A and Supplemental Table S3).

236 We identified 89 JA-related DEGs in *mob1a-2/b-1*, which include 83  
237 up-regulated and 6 down-regulated genes (Supplemental Table S4). First, the  
238 expression of many pivotal genes in JA biosynthesis, including the four *13-LOXs*,  
239 *AOS*, *AOC*, *OPR3*, and *OPCL* were dramatically up-regulated (Fig. 4B). Second,  
240 *JAR1*, *ILL6*, *IAR3*, *ST2A*, *JOX*, *CYP94B3*, and *CYP94C1* were also up-regulated,  
241 which encode enzymes that catalyze a number of key metabolic processes of JA and  
242 JA-Ile, including hydrolysis, sulfation, hydroxylation, and carboxylation (Fig. 4C).  
243 Third, five *JAZs* and *MYC2* in the JA signaling pathway were markedly up-regulated  
244 (Fig. 4D). Moreover, some genes involved in response to JA, such as *VSP2*, *TAT3*,  
245 and *JR2*, were also up-regulated (Fig. 4D, Supplement Table S4).

246 To validate the RNA-seq results, we carried out RT-qPCR analysis. The results

---

247 confirmed the increased expression of the up-regulated DEGs in *mob1a-2/b-1*  
248 compared to that in the single mutants and WT (Fig. 4E-G). Therefore, AtMOB1A  
249 and AtMOB1B likely negatively regulate JA biosynthetic, metabolic, and signaling  
250 pathways.

251

### 252 **JA content is significantly increased in the *mob1a-2/b-1* double mutant**

253 The up-regulation of many genes involved in JA biosynthesis, metabolism, and  
254 signaling in the *mob1a-2/b-1* double mutant may lead to an alteration of JA  
255 concentrations. To test this hypothesis, we measured endogenous JA contents using  
256 the gas chromatography-mass spectrometry (GC-MS) method. Indeed, JA content in  
257 the *mob1a-2/b-1* mutant was dramatically increased compared to that in the single  
258 mutants and WT plants. JA content was similar in the single mutants and WT (Fig.  
259 5A). These results suggest that AtMOB1A and AtMOB1B negatively regulate JA  
260 accumulation.

261

### 262 **The *mob1a-2/b-1* double mutant is hypersensitive to exogenous Me-JA treatment**

263 It is known that JA can promote leaf senescence (He et al., 2002; Xiao et al., 2004;  
264 Shan et al., 2011). We tested whether the *mob1* single and double mutants responded  
265 to exogenous JA treatments differently than WT. Five-d-old seedlings of WT,  
266 *mob1a-2* and *mob1b-1* single mutants, and the *mob1a-2/b-1* double mutant were  
267 transferred onto 1/2 MS plates containing different concentration (0, 10, 25, 50, 100,  
268 and 200  $\mu$ M) of Me-JA and grown for a further 14 d. The leaves of the double mutant  
269 became senescent and yellow when treated with Me-JA at 100  $\mu$ M and 200  $\mu$ M,  
270 whereas the WT and the single mutants remained green (Fig. S4). In addition,  
271 RNA-seq results indicated that several senescence-associated genes displayed altered  
272 expression in the double mutant (Table S5), including up-regulated  
273 *Senescence-associated gene 21* (*SAG21/AT4G02380*),  
274 *Senescence/dehydration-associated protein-related A* (*AT4G15450*), and  
275 *ERD7/Senescence/dehydration-associated protein-related* (*AT2G17840*), and  
276 down-regulated *Rubisco Activase (RCA)*, and *Senescence-associated family protein*

---

277 (AT1G66330). These results are consistent with the observed increase in JA content in  
278 the double mutant.

279

280 **Disruption of *MYC2* partially rescues the developmental defects and JA**  
281 **hypersensitivity of *mob1a-2/b-1***

282 The increased expression of JA-related genes and JA content in the *mob1a-2/b-1*  
283 double mutant suggested that *AtMOB1A* and *AtMOB1B* negatively regulate JA  
284 accumulation. To test the biological relevance of these observations, we analyzed the  
285 genetic interaction between *myc2-2* and the *mob1a-2/b-1* double mutant. *MYC2*  
286 encodes a key downstream transcription factor that regulates diverse aspects of JA  
287 responses, and its expression was also found to be up-regulated in *mob1a-2/b-1* (Table  
288 S4, Fig. 4G). We introduced the *myc2-2* mutation into the *mob1a-2/b-1* background  
289 by genetic crossing. The *myc2-2 mob1a-2/b-1* triple mutant developed longer roots  
290 than the *mob1a-2/b-1* double mutant (Fig. 5B-D), indicating that the *myc2-2* mutation  
291 can partially suppress the root defects of *mob1a-2/b-1*.

292 Because *MYC2* plays critical roles in activating JA-induced leaf senescence (Qi  
293 et al., 2015), we examined JA-induced senescence in the *myc2-2 mob1a-2/b-1* triple  
294 mutant. It was clear that the *myc2-2* mutation repressed the JA hypersensitivity of the  
295 *mob1a-2/b-1* double mutant. Both the morphological defects and decreased  
296 chlorophyll content of *mob1a-2/b-1* were suppressed by *myc2-2*. (Fig. 5E-F). These  
297 results suggest that the root defects and JA hypersensitivity of the *mob1a-2/b-1* double  
298 mutant are partially caused by over-accumulation of JA, and are dependent on  
299 *MYC2*-mediated JA signaling.

300

301 **Expression levels of *PLT1* and *PLT2* are decreased in the *mob1a-2/b-1* double**  
302 **mutant**

303 *PLETHORA (PLT) 1* and *PLT2* encode proteins belonging to the AP2 class of  
304 transcription factors, and are essential for root stem cell niche patterning (Aida et al.,  
305 2004; Galinha et al., 2007). It is known that *MYC2* represses the expression of *PLT1*  
306 and *PLT2*, which restricts root meristem activity and inhibits primary root growth

---

307 (Chen et al., 2011). To investigate the expression of *PLT1* and *PLT2* in *mob1a-2/b-1*,  
308 we introduced markers *pPLT1:CFP* and *pPLT2:CFP* (Galinha et al., 2007) into the  
309 mutant backgrounds by genetic crossing. The expression levels of *pPLT1:CFP* and  
310 *pPLT2:CFP* were significantly decreased in the *mob1a-2/b-1* double mutant  
311 compared to that in the single mutants and WT (Fig. 6A-D). We further introduced the  
312 *pPLT1:PLT-YFP* and *pPLT2:PLT-YFP* fusions (Galinha et al., 2007) into the mutant  
313 backgrounds by genetic crossing, and found that, in agreement, the resulting protein  
314 levels were also significantly decreased in *mob1a-2/b-1* compared to that in the single  
315 mutants and WT (Fig. 6E-H). To examine the root stem cell identity, we introduced  
316 the quiescent center (QC) marker *pWOX5::GFP* into the mutant backgrounds by  
317 genetic crossing. The GFP signals were detected in the QC cells (Fig. S5), indicating  
318 that the root stem cell identity was still maintained. These results suggest that  
319 up-regulated *MYC2* expression represses *PLT1/2* expression in the *mob1a-2/b-1*  
320 double mutant, which at least partially accounts for the root developmental defects.

321

### 322 **Genetic interaction between *mob1a-2/b-1* and *sik1* mutants**

323 It was previously reported that the Hippo/STE20 homolog SIK1 interacts with  
324 MOB1 to regulate cell proliferation and cell expansion in Arabidopsis (Xiong et al.,  
325 2016). *sik1* mutant plants are smaller than WT (Xiong et al., 2016) and the JA levels  
326 in the *sik1* mutant are decreased compared to WT (Zhang et al., 2018). We generated a  
327 *sik1 mob1a-2/b-1* triple mutant by genetic crossing, and found that seedlings of the  
328 resulting triple mutant were smaller than *mob1a-2/b-1* double-mutant seedlings (Fig.  
329 7A-C). Because JA levels are increased in *mob1a-2/b-1* but decreased in *sik1* mutant,  
330 we examined the expression of several JA-responsive genes in these mutant  
331 backgrounds. The expression levels of *JAZ1*, *JAZ2*, *JAZ5*, *JAZ9*, *JAZ19*, and *MYC2*  
332 were increased in *mob1a-2/b-1* but significantly decreased in the *sik1* mutant. The  
333 expression levels of these genes were increased in the *sik1 mob1a-2/b-1* triple mutant  
334 compared to in the *sik1* mutant (Fig. 7D). These results suggest that changes to  
335 JA-responsive gene expression caused by the *mob1a-2/b-1* mutations were partially

---

336 alleviated by the *sik1* mutation in the *sik1 mob1a-2/b-1* triple mutant, consistent with  
337 the observed differences in JA levels in *mob1a-2/b-1* and *sik1*.

338

### 339 **Discussion**

340 In this paper, we report that *AtMOB1A* and *AtMOB1B* genetically and physically  
341 interact to control Arabidopsis development. The *mob1a-2/b-1* double mutant was  
342 reduced in size with severe developmental defects, and the expression levels of many  
343 genes in the JA biosynthetic, metabolic, signaling, and responses pathways were  
344 up-regulated. Consistent with these observations, *mob1a-2/b-1* accumulated much  
345 more JA than the single mutants and WT, and the double mutant was hypersensitive to  
346 JA treatment. Disruption of the key JA signaling gene *MYC2* partially alleviated  
347 *mob1a-2/b-1* root defects and JA hypersensitivity. *mob1a-2/b-1* was associated with  
348 decreased expression of *PLT1/2*, suggesting that altered expression of these critical  
349 root development genes partially accounts for the observed root defects.

350

### 351 **AtMOB1A and AtMOB1B interact to regulate growth and development**

352 Previously, it has been shown that *AtMOB1A* is important for many plant  
353 development processes (Citterio et al., 2006; Pinoso et al., 2013; Cui et al., 2016), and  
354 that *AtMOB1A* plays critical roles in auxin-mediated development (Cui et al., 2016).  
355 Although the *mob1a* single mutant plants displayed strong developmental defects and  
356 the *mob1b* phenotype was similar to WT, *mob1a-2/b-1* showed an enhanced mutant  
357 phenotype compared to *mob1a-2* and *mob1b-1*, indicating that *AtMOB1A* and  
358 *AtMOB1B* have unique and overlapping functions. Interestingly, such genetic  
359 interaction and redundant or overlapping function of MOB1A/B were also observed  
360 in mouse. The mouse *mob1a/b* double mutant exhibited embryonic lethality or severe  
361 cancer susceptibility (Nishio et al., 2012). *Mob1a/1b* double mutation in mouse liver  
362 resulted in death within 3 weeks of birth or liver cancers and death by age 60 weeks  
363 (Nishio et al., 2016).

364 On the other hand, *AtMOB1A* and *AtMOB1B* proteins physically interact in vivo.  
365 The interaction between hMOB1A and hMOB1B was also reported in humans (Wang

---

366 et al., 2014), suggesting that the interaction between these two proteins is also  
367 conserved. Previously, it was reported that Arabidopsis serine/threonine kinase 1  
368 (SIK1) is a Hippo homolog, and that AtMOB1A and AtMOB1B interact with SIK1  
369 (Xiong et al., 2016). These genetic and physical interactions suggest that SIK1,  
370 AtMOB1A, and AtMOB1B form a large protein complex. Interestingly, the *sik1*  
371 *mob1a-2/b-1* triple mutant displayed stronger developmental defects compared to the  
372 *mob1a-2/b-1* double mutant, suggesting that there might be additional components  
373 involved in regulating the affected developmental processes. There are 10 *SIK1*-like  
374 genes in the MAP4 Kinase family (Zhang et al., 2018). It is possible that other  
375 members of the MAP4 family play redundant roles with SIK1. Recently, it was shown  
376 that SIK1 associates with, phosphorylates, and stabilizes the central immune regulator  
377 BIK1 (Zhang et al., 2018). On the other hand, MOB1s are adaptor/scaffolding  
378 proteins. It is not clear whether SIK1 phosphorylates MOB1 and/or MOB1 activates  
379 SIK1 kinase activity.

380 Because the phenotypes of the *mob1a-2/b-1* double mutant are stronger than those  
381 of the *mob1a-2* and *mob1b-1* single mutants, it is likely that AtMOB1B and  
382 AtMOB1A proteins also form homodimer/oligomers. Also, because the *mob1a-2*  
383 mutant displayed strong developmental defects whereas *mob1b-1* was largely normal,  
384 it is likely that AtMOB1A plays the dominant role. Indeed, a total of 11 AtMOB1A/B  
385 peptide sequences were detected as AtMOB1A-interacting proteins. Nine of these  
386 were shared by AtMOB1A/B, and the remaining two were AtMOB1B specific (Table  
387 S1). These results indicate AtMOB1A and AtMOB1B interacted in the IP-MS assay in  
388 Arabidopsis, and further suggest that AtMOB1A and AtMOB1B form  
389 homodimer/oligomers.

390

### 391 **AtMOB1A and AtMOB1B modulate JA accumulation**

392 JAs are important in regulating plant growth and development as well as plant  
393 responses to biotic and abiotic stresses. JA inhibits primary root growth and promotes  
394 leaf senescence (Huang et al., 2017). We found that *mob1a-2/b-1* mutant plants had a  
395 very small growth habit, with small cotyledons and short roots. It was reported that JA

---

396 treatment markedly reduces the expression of *CYCB1;1:GUS* and represses cell  
397 division activity in Arabidopsis root meristems (Chen et al., 2011). We showed that  
398 the expression of *CYCB1;1:GUS* was dramatically decreased in *mob1a-2/b-1* mutant  
399 plants (Fig. 2), which is consistent with their higher JA level (Fig. 5). These results  
400 suggest that the short root phenotype of the *mob1a-2/b-1* double mutant could be  
401 partially caused by JA-induced repression of root cell division.

402 The expression levels of many genes involved in JA biosynthetic, metabolic, and  
403 signaling pathways were increased, and JA content was elevated in *mob1a-2/b-1*.  
404 Moreover, the expression of *MYC2* was increased and the expression of *PLT1/2* was  
405 decreased in the double-mutant plants. These observations are consistent with the  
406 findings that JA reduces the expression levels of *PLT1* and *PLT2*, which is mediated  
407 by the direct binding of *MYC2* to the promoters of *PLT1* and *PLT2* to repress their  
408 expression (Chen et al., 2011). Moreover, disruption of *MYC2* in the *mob1a-2/b-1*  
409 background partially alleviated the short-root phenotype, suggesting that the root  
410 defects were at least partially caused by increased endogenous JA. The *mob1a-2/b-1*  
411 double mutant was hypersensitive to exogenous Me-JA treatment in terms of leaf  
412 senescence. JA-repressed *RCA*, which plays an important role in JA-induced leaf  
413 senescence (Shan et al., 2011), was among the few down-regulated DEGs in  
414 *mob1a-2/b-1* plants. Our RNA-seq analysis also revealed that expression of some JA  
415 responsive genes was altered in the *mob1a-2/b-1* double mutant, such as the  
416 upregulation of *VPS2*, *TAT*, and *LOX3*, the most prominent marker genes responding  
417 to wounding activated by *MYC2* in the JA signaling pathway (Titarenko et al., 1997;  
418 Lorenzo et al., 2004). More importantly, the JA hypersensitivity of the *mob1a-2/b-1*  
419 double mutant was markedly alleviated by the *myc2* mutation in *myc2-2 mob1a-2/b-1*  
420 plants. These results suggest that the elevated JA content in the *mob1a-2/b-1* double  
421 mutant caused the JA-related phenotypes. Intriguingly, disruption of *MYC2* only  
422 mildly suppressed the extreme short-root phenotype observed in *mob1a-2/b-1*,  
423 suggesting that other factors besides JA pathways, such as auxin signaling, are also  
424 involved in regulating root growth in the *mob1a-2/b-1* double mutant. This hypothesis  
425 is consistent with our previous report that *AtMOB1A* plays a role in auxin-mediated

---

426 development (Cui et al., 2016). It is likely that *AtMOB1B* plays similar roles in  
427 modulating auxin signaling.

428 Interestingly, it was reported that the expression of *JAZ* genes (*JAZ1*, *JAZ2*, *JAZ5*,  
429 *JAZ6*, *JAZ9*, and *JAZ12*), and *MYC* genes (*MYC2*, *MYC3*, and *MYC4*) was repressed  
430 in the *sik1* mutant (Xiong et al., 2016), suggesting that *SIK1* also plays roles in  
431 JA-related development. However, because the expression of some of the *JAZs* and  
432 *MYCs* in the *mob1a-2/b-1* double mutant was up-regulated, it seems that *AtMOB1A/B*  
433 and *SIK1* play different roles in modulating JA pathways. Indeed, JA levels were  
434 decreased in the *sik1* mutant compared to WT (Zhang et al., 2018), whereas they were  
435 increased in *mob1a-2/b-1* (Fig. 5A). These findings suggest that *SIK1* promotes and  
436 *MOB1A/B* represses JA levels. Consistently, the expression levels of *JAZs* and *MYC2*  
437 were increased in the *sik1 mob1a-2/b-1* triple mutant compared to in the *sik1* mutant  
438 (Fig. 7). It is intriguing how components in the same protein complex would  
439 antagonistically modulate JA levels. The *sik1 mob1a-2/b-1* triple-mutant plants  
440 showed compromised regulation of JA-related genes, but displayed more severe  
441 developmental defects than *sik1* or the *mob1a-2/b-1* double mutant. These results  
442 suggest that *MOB1* and *SIK1* may function similarly in controlling cell proliferation,  
443 but may have opposite roles in regulating JA levels and JA-related gene expression.  
444 The exact molecular mechanisms for such complex regulation are not currently  
445 understood. It was reported that the *sik1* mutant exhibited significantly higher levels  
446 of basal salicylic acid (SA) and decreased levels of JA (Zhang et al., 2018). Since  
447 *SIK1* plays a role in antibacterial immunity response (Zhang et al., 2018) and *MOB1*  
448 and *SIK1* physically interact, it is possible that *MOB1* plays a role in biotic stress  
449 responses, perhaps through JA signaling.

450

## 451 **AtMOB1A and AtMOB1B act as key regulators in auxin- and JA-mediated plant** 452 **growth**

453 Previously, we reported that *AtMOB1A* plays critical roles in auxin-mediated plant  
454 development. We isolated the *mob1a/ncp1* mutant as an enhancer of *pid*, and showed  
455 that it had strong genetic interactions with mutants in auxin biosynthesis, polar

---

456 transport, and signaling (Cui et al., 2016). Disruption of *AtMOB1A* led to a reduced  
457 sensitivity to exogenous auxin. Our previous results demonstrated that *AtMOB1A*  
458 plays an important role in *Arabidopsis* development by promoting auxin signaling  
459 (Cui et al., 2016). Our results presented in this paper clearly indicate that *AtMOB1A*  
460 and *AtMOB1B* also act as key regulators of JA-mediated plant growth. It is likely that  
461 *AtMOB1A* and *AtMOB1B* physically interact with each other and are components of  
462 a large protein complex which includes *SIK1* (Xiong et al., 2016). *AtMOB1A* and  
463 *AtMOB1B* promote auxin signaling and cell proliferation; however, the two proteins  
464 repress JA accumulation. Thus, the *AtMOB1*-containing protein complex likely  
465 regulates the crosstalk between auxin- and JA-mediated plant growth and  
466 development. A molecular framework for JA-induced inhibition of root growth  
467 through interaction with auxin pathways is well established, in which  
468 *MYC2*-mediated repression of *PLT* expression integrates JA action into the auxin  
469 pathway in regulating root meristem activity and stem cell niche maintenance (Chen  
470 et al., 2011). Auxin upregulates *PLT1* and *PLT2* transcripts and positively regulates  
471 stem cell niche maintenance and meristem activity (Aida et al., 2004), and JA  
472 downregulates *PLT1* and *PLT2* expression and negatively regulates stem cell niche  
473 maintenance and meristem activity (Chen et al., 2011). We showed that *PLT1/2*  
474 expression is repressed in the *mob1a-2/b-1* double mutant, which could be an  
475 integrative outcome of elevated JA content and reduced auxin signaling. It would be  
476 interesting to further explore the mechanisms by which *AtMOB1A/B* control JA  
477 accumulation and the crosstalk with auxin signaling.

478

## 479 **Materials and Methods**

480

### 481 **Plant materials and growth condition**

482 All *Arabidopsis thaliana* materials used in this work were in the Col-0 ecotype  
483 background. Seeds were surface sterilized for 15 min in 70% (v/v) and then 100%  
484 (v/v) ethyl alcohol. The seeds were then sowed on half-strength Murashige and Skoog  
485 (1/2 MS) medium containing 0.8% (w/v) agar. The plates were transferred to 4°C for

---

486 3 d in darkness for vernalization. Plants were grown at 22°C under a 16-h light/8-h  
487 dark cycle. The T-DNA insertion lines, including *mob1 a-2* (GK\_719G04), *mob1 b-1*  
488 (SALK\_062070), and *mob1 d-1* (SALK\_053800) were purchased from the NASC.  
489 The *mob1 a-2* (GK\_719G04) mutant was genotyped as described previously (Cui et  
490 al., 2016). For genotyping *mob1 b-1* (SALK\_062070), the primers  
491 5'-GGATGAAGTGTGTTGAAGC-3' and 5'-GCTGAGTAATGG TTGTGA-3'  
492 combined with JMLB1 were used. For genotyping *mob1 d-1* (SALK\_053800), the  
493 primers 5'-GGGCAAAGTCCAAATCCT-3' and 5'-CCGCTTCACGAAATCCTC-3'  
494 combined with JMLB1 were used.

495

#### 496 **DNA constructs and plant transformation**

497 For the expression patterns of *ATMOB1B*, the plasmid was constructed with its  
498 genomic DNA fragment containing the coding region alongside up- and down-stream  
499 regulatory sequences with the GFP or GUS gene inserted before the stop code. The  
500 *AtMOB1B* gene was divided into parts A and B. The part A was amplified using  
501 primers 5'-CGGGGTACCGCAGGAATACTATTGGGCCTG-3' and  
502 5'-ACTGGGCCCCGTAAGGTGCAATGATAGATTC-3'. The part B was amplified  
503 using primers 5'-ACTGGGCCCACCAAACAAAACCCAAATCCTC-3' and  
504 5'-ACTGTCGACGGCTCCAACACAAAATACCTC-3'. The two PCR products  
505 were double digested with *KpnI* and *Apa I*, or *ApaI* and *SallI*, respectively, and cloned  
506 into the *KpnI-SallI* sites of vector *pPZP211* to generate *pPZP211-gAtMOB1B*  
507 construct. The GUS or GFP gene was inserted immediately before the stop code using  
508 restriction site of *ApaI*. The *pPZP211-gAtMOB1B-GUS* or  
509 *pPZP211-gAtMOB1B-GFP* construct was transformed into *Agrobacterium*  
510 *tumefaciens* strain GV3101, and then Arabidopsis plants were transformed by floral  
511 dipping. The transgenic seedlings were selected on 1/2 MS plates with 50 µg/mL  
512 kanamycin. The *pPZP211-gAtMOB1A* (Cui et al., 2016) and  
513 *pPZP211-gAtMOB1B-GFP* constructs were used in the complementation experiments  
514 of the *mob1a-2/b-1* mutants (Fig. S3).

515

---

516 **Phenotypic analysis, statistical analysis, and microscopy**

517 Seedlings and roots were photographed and their lengths were measured using NIH  
518 ImageJ software (<https://imagej.nih.gov/ij/>). Seedlings were mounted in HCG  
519 (H<sub>2</sub>O-Chloral hydrate-Glycerine) solution (Chloral hydrate:water:glycerol = 8:3:1)  
520 and the root meristem cells analyzed on a Leica microsystems DM4500B microscope.  
521 Statistical significance was evaluated by Student's *t*-test analysis or one-way ANOVA  
522 analysis followed by LSD test (SPSS). Histochemical staining for GUS activity in  
523 plants was performed as described previously (Cui et al., 2016). For the Lugol  
524 staining, roots were incubated in the Lugol solution for 3–5 min, and then washed in  
525 water once, and mounted in HCG solution for microscopy analysis. GFP, YFP, CFP,  
526 and FM4-64 fluorescence was imaged under a confocal laser scanning microscope  
527 Olympus FV1000MPE following the manufacturer's instructions. The fluorescence  
528 intensities were measured using ImageJ for quantification analysis.

529

530

531 **Co-IP assays and Mass Spectrometry**

532 For the Co-IP assay of AtMOB1A and AtMOB1B, *pSuper1300:AtMOB1A-Flag*  
533 and *pEarleyGate 104-35S:YFP-AtMOB1B* plasmids were constructed and introduced  
534 into *Agrobacterium tumefaciens* strain GV3101, then *Nicotiana benthamiana* leaves  
535 were transformed by injection. Leaves were ground in liquid nitrogen and proteins  
536 were extracted with same volume of extraction buffer [100 mM HEPES (pH 7.5), 5  
537 mM EDTA, 5 mM EGTA, 10 mM NaF, 5% (v/v) Glycerol, 10 mM Na<sub>3</sub>VO<sub>4</sub>, 10 mM  
538 DTT, 1 mM PMSF, 0.1% (v/v) Triton X-100, protease inhibitor cocktail (Sigma)].  
539 Samples were mixed twice quickly following incubating on ice for 30 min and then  
540 centrifuged at 14000 *g* at 4°C for 30 min. The supernatant was incubated with  
541 anti-Flag agarose (Sigma) or Anti-GFP-mAb agarose (MBL) in IP buffer [20 mM  
542 Tris-HCl (pH 7.5), 150 mM NaCl, 1 mM EDTA, 1 mM EGTA, 1 mM Na<sub>3</sub>VO<sub>4</sub>, 1 mM  
543 NaF, 10 mM β-glycerophosphate, 0.1% (v/v) Triton X-100, protease inhibitor cocktail  
544 (Sigma)] at 4°C for 2 h with gentle shaking. The agarose was collected and washed  
545 three times with PBS, boiled in 2×SDS loading buffer for 5 min and examined by

---

546 immunoblot analysis with anti-GFP (CWBIO) or anti-Flag (Abmart) antibodies.  
547 For Mass Spectrometry, *pSuper1300:AtMOB1A-Flag* vector was introduced into  
548 *Agrobacterium*. *Arabidopsis* plants were transformed by the floral dipping method. T4  
549 generation transgenic plants were used for extracting total protein and IP using the  
550 method described above. The AtMOB1A interacting proteins were examined by Mass  
551 Spectrometry.

552

### 553 **LCI assay**

554 The LCI assay was performed as previously described (Chen et al., 2008). *A.*  
555 *tumefaciens* bacteria strain GV3101 containing *pCAMBIA1300-AtMOB1A-nLUC*,  
556 *pCAMBIA1300-cLUC-AtMOB1B*, *pCAMBIA1300-nLUC*, and *pCAMBIA1300-cLUC*  
557 were injected into *N. benthamiana* leaves. The empty cLUC and nLUC vectors were  
558 used as negative controls. The plants were incubated in darkness overnight, and the  
559 leaves were harvested after 2–3 d. Leaves were incubated in D-Luciferin, Potassium  
560 Salt (Goldbio) solution in darkness for 3 min and the luciferase signals were analyzed  
561 with a Tanon 5200 Chemiluminescent Imaging System (Tanon, Shanghai, China). The  
562 imaging exposure time was 3 min. Eight leaves were analyzed for each experiment,  
563 with three biological replicates in total.

564

### 565 **RNA Extraction, RT-qPCR, and RNA-Seq**

566 The samples were collected from 10-d-old whole seedlings of Col-0, *mob1a-2*,  
567 *mob1b-1*, and *mob1a-2 b-1*. Total RNA was extracted using a Biozol kit (Biomiga)  
568 according to the manufacturer's instructions. The first-strand cDNA synthesis was  
569 performed using M-MLV Reverse Transcriptase (Promega). The qPCR analysis was  
570 performed using a light cycle 96 (Roche) and SYBR Green I (Takara). *ACTIN2*  
571 (*AT3G18780*) was used as an internal control. All experiments were performed with  
572 three independent biological replicates. Statistical significance was evaluated by  
573 one-way ANOVA analysis (multiple comparison by Tukey post test). The primers  
574 used for RT-qPCR analysis are listed in Table S6.

575 For RNA-seq, mRNA enrichment, cDNA library construction, and single-end

---

576 sequencing were performed by BGI ([www.genomics.org.cn](http://www.genomics.org.cn)). Filtered Clean-reads  
577 were mapped to the reference genome (TAIR10) available at TAIR  
578 (<http://www.arabidopsis.org>). The gene expression quantitation was calculated using  
579 the RSEM tool (Li and Dewey, 2011). The DEGs were selected according the  
580 threshold value fold change  $\geq 2$  ( $\log_2$  ratio  $\geq 1.0$ ) and deviation probability  $\geq 0.7$   
581 through comparing the gene expression quantitation of mutants and wild-type. GO  
582 enrichment analysis was carried out using AmiGO 2 program  
583 (<http://amigo.geneontology.org/amigo>).

584

### 585 **Measurement of endogenous JA by GC-MS**

586 Fourteen-d-old whole plants of every genotype were collected in triplicate  
587 replicates. The samples were homogenized quickly in liquid N<sub>2</sub>, then powdered  
588 samples were weighed dry-frozen. Samples were extracted with 80% (v/v) methanol  
589 containing 0.2 ng [<sup>2</sup>H<sub>6</sub>]JA as an internal standard and incubated overnight at 4°C.  
590 After centrifugation at 5,976 g for 5 min, the supernatant layer was collected in new  
591 glass tubes and dried with nitrogen gas. The samples were dissolved in 2.5%  
592 (v/v)ethyl acetate and the supernatant were dried with nitrogen gas. Following the  
593 addition of 23% (v/v) methanol and incubation for 2 h at -20°C, samples were  
594 centrifuged at 10,625 g for 7 min and the supernatant was dried with nitrogen gas.  
595 Samples were dissolved in 30  $\mu$ l BSTFA with 3  $\mu$ l pyridine and incubated for 30 min  
596 at 80°C, then analyzed using GC-MS (7890A-7000B, Agilent, USA). The amount of  
597 JA present in plant samples was calculated based on the internal standards and weight  
598 of the tissues and retention time.

599

### 600 **Measurement of chlorophyll content**

601 Measurement of chlorophyll content was performed as previously described (Qi et al.,  
602 2015). The leaves was detached and weight. For chlorophyll extraction, the leaves  
603 were incubated in 80% (v/v) acetone in the dark. Absorbances were measured at 645  
604 and 663 nm using a spectrophotometer (Beckman Coulter DU-800). Chlorophyll  
605 contents were calculated and expressed as a ratio of the chlorophyll content of Col-0

---

606 treated with mock.

607

608 **Accession numbers**

609 Sequence data from this article can be found in the GenBank/EMBL data libraries

610 under accession numbers JAZ1 (AT1G19180), JAZ2 (AT1G74950), JAZ3

611 (AT3G17860), JAZ4 (AT1G48500), JAZ5 (AT1G17380), JAZ6 (AT1G72450), JAZ7

612 (AT2G34600), JAZ8 (AT1G30135), JAZ9 (AT1G70700), JAZ10 (AT5G13220),

613 JAZ11 (AT3G43440), and JAZ12 (AT5G20900).

614 .

615 **Supplemental Data**

616 **Supplemental Figure S1.** Analysis of T-DNA insertion lines of *AtMOB1* genes and

617 generation of CRISPR line of *AtMOB1C*.

618 **Supplemental Figure S2.** Representative images of 21-d-old plants of Col-0,

619 *mob1a-2*, *mob1b-1*, and *mob1a-2/b-1* mutants.

620 **Supplemental Figure S3.** Complementation of *mob1a-2/b-1* with a genomic DNA

621 fragment of *AtMOB1A* or *AtMOB1B*.

622 **Supplemental Figure S4.** Expression patterns of *AtMOB1A* and *AtMOB1B* and

623 subcellular localization of the proteins.

624 **Supplemental Figure S5.** JA treatment of seedlings at different concentrations.

625 **Supplemental Figure S6.** *pWOX5:GFP* expression in the root of 6-d-old seedlings.

626 **Supplemental Table S1.** *MOB1B* was identified by IP-MS assays in *MOB1A*-Flag

627 transgenic plants.

628 **Supplemental Table S2.** List of differentially expressed genes (DEGs).

629 **Supplemental Table S3.** Enriched GO categories in biological process of the DEGs.

630 **Supplemental Table S4.** DEGs involved in JA related pathway.

---

631 **Supplemental Table S5.** DEGs involved in leaf senescence.

632 **Supplemental Table S6.** Primers used for RT-qPCR reactions.

633

### 634 **Acknowledgements**

635 We thank Drs. Yunde Zhao for critical reading of the manuscript, Daoxin Xie and  
636 Susheng Song for providing the *myc2* mutant seeds, Qingqiu Gong for *sik1* mutant  
637 seeds, Yuxin Hu for the Chemiluminescent Imaging System, Jianmin Zhou for the  
638 LCI system vectors, Li-jia Qu for insightful discussion. We thank Ms. Lu Wang, and  
639 Ms. Jingquan Li from the Plant Science Facility of the Institute of Botany, Chinese  
640 Academy of Sciences, for their excellent technical assistance.

641

### 642 **Figure legends**

643

#### 644 **Figure 1. Analysis of loss-of-function *atmob1* mutants.**

645 (A) A phylogenetic tree of AtMOB1 family proteins. (B) Schematic representation of  
646 *AtMOB1* gene structures and positions of the T-DNA insertion. The 5-bp deletion in  
647 *mob1c-2* mutant was designated as “Del-agGAG” in *AtMOB1C*. (C-D) 6-d-old  
648 seedlings of Col-0, *mob1a-2*, *mob1b-1*, *mob1a-2/b-1*<sup>+/-</sup>, and *mob1a-2/b-1* mutants. (E)  
649 Electron micrograph of a *mob1a-2/b-1* double-mutant seedling. (F-G) Adult plants (F)  
650 and siliques (G) of Col-0, *mob1a-2*, *mob1b-1*, and *mob1a-2/b-1*<sup>+/-</sup>. (H-K) 6-d-old  
651 seedlings of *mob1a-2/b-1* (H), *mob1a-2/b-1/c-1* (I), *mob1a-2/b-1/d-1* (J), and  
652 *mob1a-2/b-1/c-2/d-1* (K). (L) 6-d-old seedlings of Col-0, *mob1c-1*, *mob1d-1*, and  
653 *mob1c-2/d-1*. Scale bars: 5 mm (C, D), 100 μm (E, H-K).

654

#### 655 **Figure 2. The *mob1a-2 b-1* mutant displays strong defects in root tips.**

---

656 (A) The root tips of 6-d-old seedlings of Col-0, *mob1a-2*, *mob1b-1*, and *mob1a-2/b-1*  
657 mutants are shown. The meristem zone is marked with two arrowheads. (B-E)  
658 Measurements of the lengths of root elongation zone (B) and meristem (C), and cell  
659 numbers in elongation zone (D) and meristem (E). (F) Root tips of 6-d-old seedlings  
660 stained with FM4-64. (G) The columella root cap cell of 6-d-old seedlings revealed by  
661 Lugol staining. (H) *CYCB1;1:GUS* expression in the root of 6-d-old seedlings. (I)  
662 Quantification of cells with *CYCB1;1:GUS* signal in (H). Data represent means  $\pm$  SD.  
663 Different letters represent the significance at the  $P < 0.001$  level (one-way ANOVA,  
664 LSD test);  $n > 20$ . Scale bars: 200  $\mu\text{m}$  (A), 50  $\mu\text{m}$  (F-H).

665 **Figure 3. Physical interaction between AtMOB1A and AtMOB1B proteins in**  
666 **vivo.**

667 (A) Co-IP assay of AtMOB1A and AtMOB1B. AtMOB1B-GFP was  
668 immuno-precipitated by using anti-GFP agarose beads, followed by immunoblot with  
669 anti-Flag antibody, and AtMOB1A-Flag was detected. (B) LCI assays showing the  
670 interaction between MOB1A and MOB1B in *N. benthamiana* leaf cells. The left panel  
671 shows the combinations of agrobacteria containing the indicated plasmids used to  
672 co-infiltrate into different leaf regions of the right panel. Empty cLUC and nLUC  
673 vectors were used as negative controls. The experiments were carried out with three  
674 independent biological repeats.

675 **Figure 4. Expression of genes involved in JA biosynthesis, metabolism, and**  
676 **signaling are altered in the *mob1a-2/b-1* double mutant.**

677 (A) Functional assignment of the DEGs by GO enrichment analysis. Bars represent –  
678  $\lg(P \text{ value})$  and the P values were adjusted by the Bonferroni approach. (B-D) The  
679 DEGs in jasmonic acid biosynthesis (B), metabolic processes of JA and JA-Ile (C),  
680 and JA signaling pathway and response to JA (D). The Heatmap indicates the ratio  
681 being up-regulated. Scale colors represent  $\log_2(\text{ratio})$ .  $\alpha$ -LeA,  $\alpha$ -linolenic acid;  
682 13-HPOT, 13-hydroperoxylinoleic acid; 12,13-EOT, 12,13-epoxyoctadecatrienoic

---

683 acid; OPDA, 12-oxophytodienoic acid; OPC-8,  
684 3-oxo-2-(2-pentenyl)-cyclopentane-1-octanoic acid; PLA1, phospholipase A1;  
685 13-LOX, 13-lipoxygenase; AOS, allene oxide synthase; AOC, allene oxide cyclase;  
686 OPR, OPDA reductase; OPCL, OPC-8-CoA ligase; ST2A, 12-OH-JA sulfotransferase;  
687 JOX, jasmonic acid oxidase; JAR1, jasmonoyl isoleucine synthase; ILL6 and IAR3,  
688 IAA-amino acid hydrolase; CYP94C1; 12-OH-JA-Ile carboxylase; JAZ,  
689 jasmonate-zim-domain protein; MYC2, bHLH zip transcription factor; VSP2,  
690 vegetative storage protein 2; TAT3, tyrosine aminotransferase 3; JR2, jasmonic acid  
691 responsive 2; RAP2.6L, ERF/AP2 transcription factor; ANAC081, Arabidopsis NAC  
692 domain containing protein 81. (E-G) Relative expression of the DEGs in JA  
693 biosynthesis (E), metabolism (F), and signaling (G) in Col-0, *mob1a-2*, *mob1b-1*, and  
694 *mob1a-2/b-1*. 10-d-old seedlings were collected for RNA extraction and RT-qPCR  
695 analysis. *ACTIN2* was used as an internal control. The expression levels of the  
696 indicated genes in Col-0 were set to 1. Error bars represent the SD of three biological  
697 repeats. Different letters indicate significant difference at  $P < 0.001$  (one-way ANOVA,  
698 Tukey post test).

699 **Figure 5. AtMOB1A and AtMOB1B negatively regulate JA accumulation.**

700 (A) Measurement of the JA contents in seedlings of Col-0, *mob1a-2*, *mob1b-1*, and  
701 *mob1-2/b-1* mutants by using GC-MS. Seedlings were grown on 1/2 MS medium for  
702 14 d after germination. Data represent means  $\pm$  SD of three independent biological  
703 repeats. Different letters represent statistical significance at the  $P < 0.001$  level  
704 (one-way ANOVA, LSD test). (B-C) 6-d-old seedlings of Col-0, *myc2-2*,  
705 *mob1a-2/b-1*, and *myc2-2 mob1a-2/b-1* mutants. Seedlings were grown on 1/2 MS  
706 medium for 6 d after germination. Scale bars: 2 mm (B), 1 mm (C). (D) Measurement  
707 of root length of Col-0, *myc2-2*, *mob1a-2/b-1*, and *myc2-2 mob1a-2/b-1* mutants. Data  
708 represent means  $\pm$  SD ( $n \geq 20$ ) with significant differences determined by Student's  
709 *t*-test. \*\*\* $P < 0.001$  compared to *mob1-2 b-1*. (E) *mob1a-2/b-1* mutants were  
710 hypersensitive to exogenous JA treatment. 5-d-old seedlings grown on 1/2 MS plates

---

711 were transferred to the 1/2 MS plates without (Control, upper panels) or with (JA,  
712 lower panels) 100  $\mu$ M Me-JA and grown for 2 weeks. Scale bars: 2 mm. (F)  
713 Measurement of chlorophyll contents. The chlorophyll contents of indicated mutants  
714 are relative to that in Col-0, which was set to 1.0. Data represent means  $\pm$  SD (n = 15).  
715 Student's *t*-test. \*\*\*P < 0.001 compared to control.

716 **Figure 6. Expression levels of *PLT1* and *PLT2* are reduced in *mob1a-2/b-1*.**

717 (A, C, E, G) Representative expression of *PLT1:CFP* (A), *PLT2:CFP* (C),  
718 *PLT1:PLT1-YFP* (E), and *PLT2:PLT2-YFP* (G) in the root tips of 6-d-old Col-0,  
719 *mob1a-2*, *mob1b-1*, and *mob1a-2/b-1* mutant seedlings. Scale bars: 50  $\mu$ m. (B, D, F,  
720 H) Quantification of CFP (A, C) and YFP (E, G) fluorescence, respectively. The  
721 fluorescence strength of Col-0 was set to 1. Data represent means  $\pm$  SD (n = 15).  
722 Different letters represent statistical significance at the P < 0.001 level (one-way  
723 ANOVA, LSD test).

724

725 **Figure 7. Genetic interaction between *MOBIA/B* and *SIK1*.**

726 (A-B) 12-d-old seedlings of Col-0, *sik1-1*, *mob1a-2/b-1*, and *mob1a-2/b-1 sik1-1*  
727 mutants. (C) Close-up of seedlings in (B). Note the triple mutant was smaller than the  
728 double mutant. Scale bars: 2 mm (A-C). (D) Relative expression of JA  
729 signaling-related genes in 12-d-old seedlings of Col-0, *mob1a-2/b-1*, *sik1-1*, and  
730 *mob1a-2/b-1 sik1-1*. *ACTIN2* was used as an internal control. The expression levels of  
731 the indicated genes in Col-0 were set to 1. Different letters indicate significant  
732 difference at P < 0.001 (n = 3, one-way ANOVA, Tukey post test).

733

734

735

736

---

737 **REFERENCES**

738

739 **Aida M, Beis D, Heidstra R, Willemsen V, Blilou I, Galinha C, Nussaume L, Noh YS, Amasino R,**  
740 **Scheres B** (2004) The PLETHORA genes mediate patterning of the Arabidopsis root stem cell  
741 niche. *Cell* **119**: 109-120

742 **Chen H, Zou Y, Shang Y, Lin H, Wang Y, Cai R, Tang X, Zhou JM** (2008) Firefly luciferase  
743 complementation imaging assay for protein-protein interactions in plants. *Plant Physiol* **146**:  
744 368-376

745 **Chen Q, Sun J, Zhai Q, Zhou W, Qi L, Xu L, Wang B, Chen R, Jiang H, Qi J, Li X, Palme K, Li**  
746 **C** (2011) The basic helix-loop-helix transcription factor MYC2 directly represses  
747 PLETHORA expression during jasmonate-mediated modulation of the root stem cell niche in  
748 Arabidopsis. *Plant Cell* **23**: 3335-3352

749 **Chow A, Hao Y, Yang X** (2010) Molecular characterization of human homologs of yeast MOB1. *Int J*  
750 *Cancer* **126**: 2079-2089

751 **Citterio S, Piatti S, Albertini E, Aina R, Varotto S, Barcaccia G** (2006) Alfalfa Mob1-like proteins  
752 are involved in cell proliferation and are localized in the cell division plane during cytokinesis.  
753 *Exp Cell Res* **312**: 1050-1064

754 **Colon-Carmona A, You R, Haimovitch-Gal T, Doerner P** (1999) Technical advance: spatio-temporal  
755 analysis of mitotic activity with a labile cyclin-GUS fusion protein. *Plant J* **20**: 503-508

756 **Cui X, Guo Z, Song L, Wang Y, Cheng Y** (2016) NCP1/AtMOB1A Plays Key Roles in  
757 Auxin-Mediated Arabidopsis Development. *PLoS Genet* **12**: e1005923

758 **Galinha C, Hofhuis H, Luijten M, Willemsen V, Blilou I, Heidstra R, Scheres B** (2007)  
759 PLETHORA proteins as dose-dependent master regulators of Arabidopsis root development.  
760 *Nature* **449**: 1053-1057

761 **Galla G, Zenoni S, Marconi G, Marino G, Botton A, Pinosa F, Citterio S, Ruperti B, Palme K,**  
762 **Albertini E, Pezzotti M, Mau M, Sharbel TF, De Storme N, Geelen D, Barcaccia G** (2011)  
763 Sporophytic and gametophytic functions of the cell cycle-associated Mob1 gene in  
764 Arabidopsis thaliana L. *Gene* **484**: 1-12

765 **Gao X, Chen J, Dai X, Zhang D, Zhao Y** (2016) An Effective Strategy for Reliably Isolating  
766 Heritable and Cas9-Free Arabidopsis Mutants Generated by CRISPR/Cas9-Mediated Genome  
767 Editing. *Plant Physiol* **171**: 1794-1800

768 **Goto H, Nishio M, To Y, Oishi T, Miyachi Y, Maehama T, Nishina H, Akiyama H, Mak TW,**  
769 **Makii Y, Saito T, Yasoda A, Tsumaki N, Suzuki A** (2018) Loss of Mob1a/b in mice results  
770 in chondrodysplasia due to YAP1/TAZ-TEAD-dependent repression of SOX9. *Development*  
771 **145**

772 **Hansen CG, Moroishi T, Guan KL** (2015) YAP and TAZ: a nexus for Hippo signaling and beyond.  
773 *Trends Cell Biol* **25**: 499-513

774 **Harvey KF, Zhang X, Thomas DM** (2013) The Hippo pathway and human cancer. *Nat Rev Cancer* **13**:  
775 246-257

776 **He Y, Fukushige H, Hildebrand DF, Gan S** (2002) Evidence supporting a role of jasmonic acid in  
777 Arabidopsis leaf senescence. *Plant Physiol* **128**: 876-884

778 **Huang H, Liu B, Liu L, Song S** (2017) Jasmonate action in plant growth and development. *J Exp Bot*  
779 **68**: 1349-1359

780 **Lai ZC, Wei X, Shimizu T, Ramos E, Rohrbaugh M, Nikolaidis N, Ho LL, Li Y** (2005) Control of

---

781 cell proliferation and apoptosis by mob as tumor suppressor, mats. *Cell* **120**: 675-685

782 **Li B, Dewey CN** (2011) RSEM: accurate transcript quantification from RNA-Seq data with or without

783 a reference genome. *BMC Bioinformatics* **12**: 323

784 **Lorenzo O, Chico JM, Sanchez-Serrano JJ, Solano R** (2004) JASMONATE-INSENSITIVE1

785 encodes a MYC transcription factor essential to discriminate between different

786 jasmonate-regulated defense responses in Arabidopsis. *Plant Cell* **16**: 1938-1950

787 **Luca FC, Winey M** (1998) MOB1, an essential yeast gene required for completion of mitosis and

788 maintenance of ploidy. *Mol Biol Cell* **9**: 29-46

789 **Nishio M, Hamada K, Kawahara K, Sasaki M, Noguchi F, Chiba S, Mizuno K, Suzuki SO, Dong**

790 **Y, Tokuda M, Morikawa T, Hikasa H, Eggenschwiler J, Yabuta N, Nojima H, Nakagawa**

791 **K, Hata Y, Nishina H, Mimori K, Mori M, Sasaki T, Mak TW, Nakano T, Itami S, Suzuki**

792 **A** (2012) Cancer susceptibility and embryonic lethality in Mob1a/1b double-mutant mice. *J*

793 *Clin Invest* **122**: 4505-4518

794 **Nishio M, Sugimachi K, Goto H, Wang J, Morikawa T, Miyachi Y, Takano Y, Hikasa H, Itoh T,**

795 **Suzuki SO, Kurihara H, Aishima S, Leask A, Sasaki T, Nakano T, Nishina H, Nishikawa**

796 **Y, Sekido Y, Nakao K, Shin-Ya K, Mimori K, Suzuki A** (2016) Dysregulated YAP1/TAZ

797 and TGF-beta signaling mediate hepatocarcinogenesis in Mob1a/1b-deficient mice. *Proc Natl*

798 *Acad Sci U S A* **113**: E71-80

799 **Pan D** (2010) The hippo signaling pathway in development and cancer. *Dev Cell* **19**: 491-505

800 **Pinosa F, Begheldo M, Pasternak T, Zermiani M, Paponov IA, Dovzhenko A, Barcaccia G,**

801 **Ruperti B, Palme K** (2013) The Arabidopsis thaliana Mob1A gene is required for organ

802 growth and correct tissue patterning of the root tip. *Ann Bot* **112**: 1803-1814

803 **Qi T, Wang J, Huang H, Liu B, Gao H, Liu Y, Song S, Xie D** (2015) Regulation of

804 Jasmonate-Induced Leaf Senescence by Antagonism between bHLH Subgroup IIIe and IIIc

805 Factors in Arabidopsis. *Plant Cell* **27**: 1634-1649

806 **Shan X, Wang J, Chua L, Jiang D, Peng W, Xie D** (2011) The role of Arabidopsis Rubisco activase

807 in jasmonate-induced leaf senescence. *Plant Physiol* **155**: 751-764

808 **Titarenko E, Rojo E, Leon J, Sanchez-Serrano JJ** (1997) Jasmonic acid-dependent and -independent

809 signaling pathways control wound-induced gene activation in Arabidopsis thaliana. *Plant*

810 *Physiol* **115**: 817-826

811 **Vitulo N, Vezzi A, Galla G, Citterio S, Marino G, Ruperti B, Zermiani M, Albertini E, Valle G,**

812 **Barcaccia G** (2007) Characterization and evolution of the cell cycle-associated mob

813 domain-containing proteins in eukaryotes. *Evol Bioinform Online* **3**: 121-158

814 **Wang W, Li X, Huang J, Feng L, Dolinta KG, Chen J** (2014) Defining the protein-protein

815 interaction network of the human hippo pathway. *Mol Cell Proteomics* **13**: 119-131

816 **Wasternack C, Song S** (2017) Jasmonates: biosynthesis, metabolism, and signaling by proteins

817 activating and repressing transcription. *J Exp Bot* **68**: 1303-1321

818 **Xiao S, Dai L, Liu F, Wang Z, Peng W, Xie D** (2004) COS1: an Arabidopsis coronatine insensitive1

819 suppressor essential for regulation of jasmonate-mediated plant defense and senescence. *Plant*

820 *Cell* **16**: 1132-1142

821 **Xiong J, Cui X, Yuan X, Yu X, Sun J, Gong Q** (2016) The Hippo/STE20 homolog SIK1 interacts

822 with MOB1 to regulate cell proliferation and cell expansion in Arabidopsis. *J Exp Bot* **67**:

823 1461-1475

824 **Zeng W, Dai X, Sun J, Hou Y, Ma X, Cao X, Zhao Y, Cheng Y** (2018) Modulation of auxin

---

825 signaling and development by polyadenylation machinery. *Plant Physiol*  
826 **Zhang M, Chiang YH, Toruno TY, Lee D, Ma M, Liang X, Lal NK, Lemos M, Lu YJ, Ma S, Liu J,**  
827 **Day B, Dinesh-Kumar SP, Dehesh K, Dou D, Zhou JM, Coaker G** (2018) The MAP4  
828 Kinase SIK1 Ensures Robust Extracellular ROS Burst and Antibacterial Immunity in Plants.  
829 *Cell Host Microbe* **24**: 379-391 e375  
830

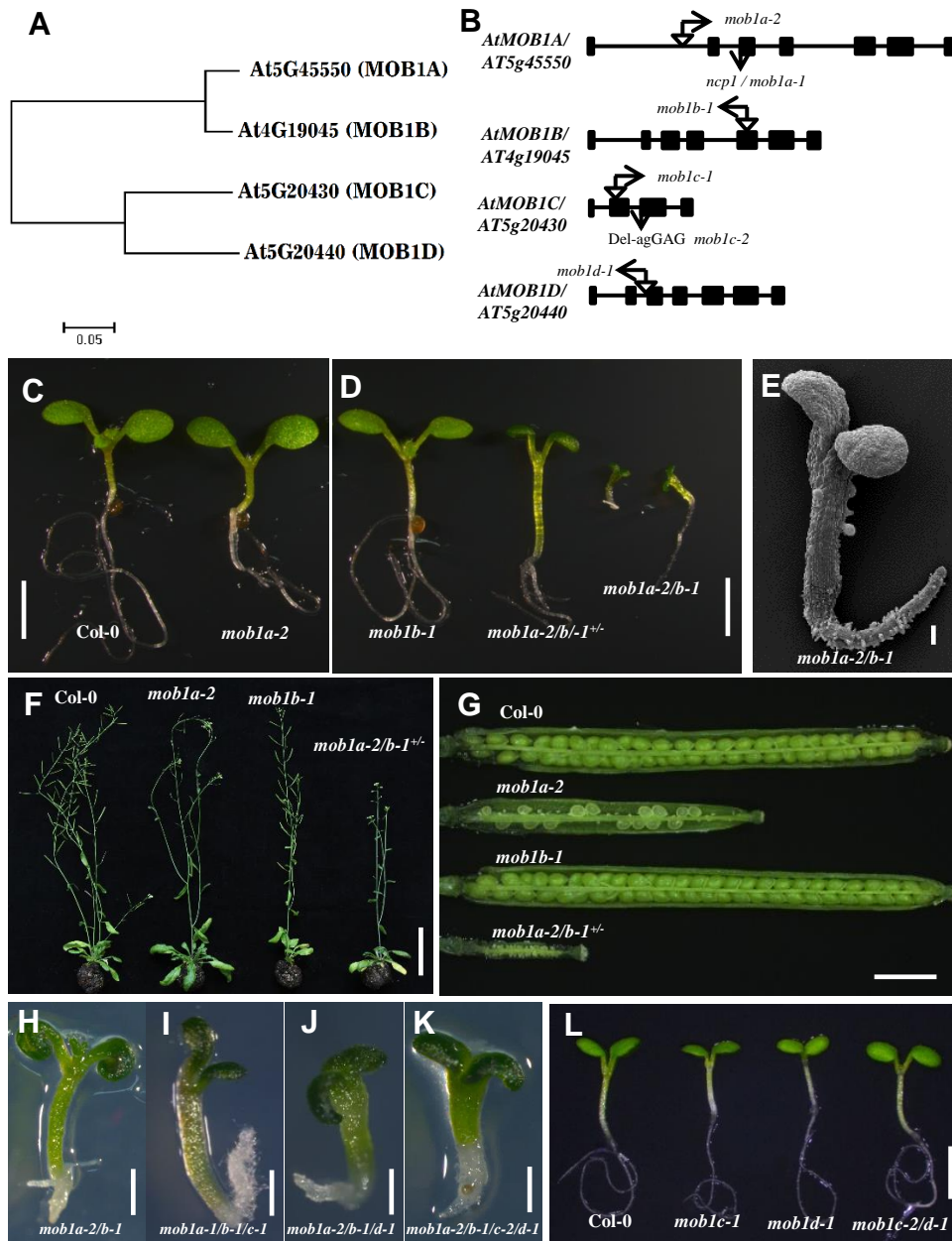


### Figure 1. Analysis of loss-of-function *atmob1* mutants.

(A) A phylogenetic tree of AtMOB1 family proteins. (B) Schematic representation of AtMOB1 gene structures and positions of the T-DNA insertion. The 5-bp deletion in *mob1c-2* mutant was designated as “Del-agGAG” in AtMOB1C. (C-D) 6-d-old seedlings of Col-0, *mob1a-2*, *mob1b-1*, *mob1a-2/b-1<sup>+/-</sup>*, and *mob1a-2/b-1* mutants. (E) Electron micrograph of a *mob1a-2/b-1* double-mutant seedling. (F-G) Adult plants (F) and siliques (G) of Col-0, *mob1a-2*, *mob1b-1*, and *mob1a-2/b-1<sup>+/-</sup>*. (H-K) 6-d-old seedlings of *mob1a-2/b-1* (H), *mob1a-2/b-1/c-1* (I), *mob1a-2/b-1/d-1* (J), and *mob1a-2/b-1/c-2/d-1* (K). (L) 6-d-old seedlings of Col-0, *mob1c-1*, *mob1d-1*, and *mob1c-2/d-1*. Scale bars: 5 mm (C, D), 100  $\mu$ m (E, H-K).

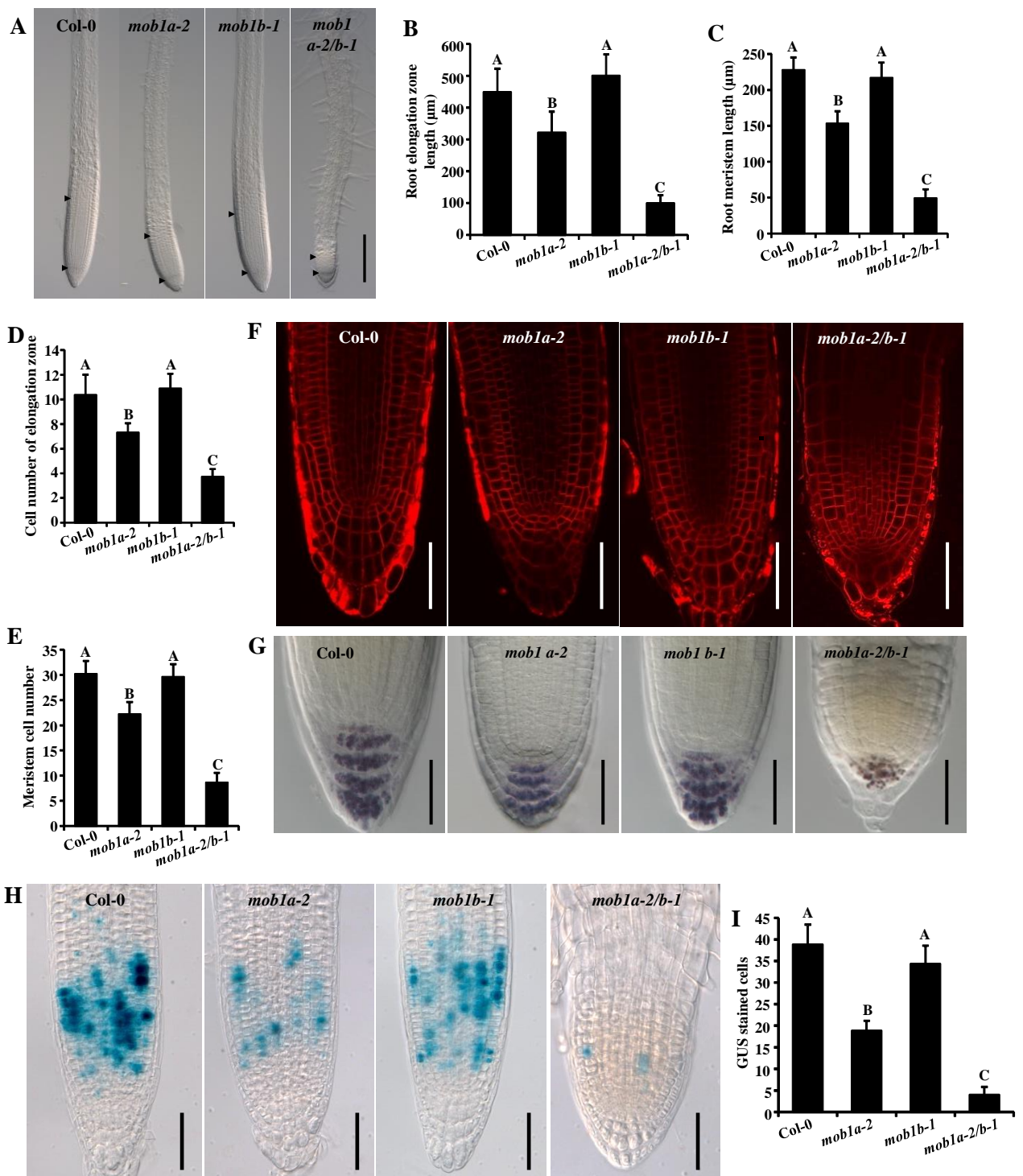


**Figure 2. The *mob1a-2 b-1* mutant displays strong defects in root tips.**

(A) The root tips of 6-d-old seedlings of Col-0, *mob1a-2*, *mob1b-1*, and *mob1a-2/b-1* mutants are shown. The meristem zone is marked with two arrowheads. (B-E) Measurements of the lengths of root elongation zone (B) and meristem (C), and cell numbers in elongation zone (D) and meristem (E). (F) Root tips of 6-d-old seedlings stained with FM4-64. (G) The columella root cap cell of 6-d-old seedlings revealed by Lugol staining. (H) *CYCB1;1:GUS* expression in the root of 6-d-old seedlings. (I) Quantification of cells with *CYCB1;1:GUS* signal in (H). Data represent means  $\pm$  SD. Different letters represent the significance at the P = 0.001 level (one-way ANOVA, LSD test);  $n > 20$ . Scale bars: 200  $\mu$ m (A), 50  $\mu$ m (F-H).

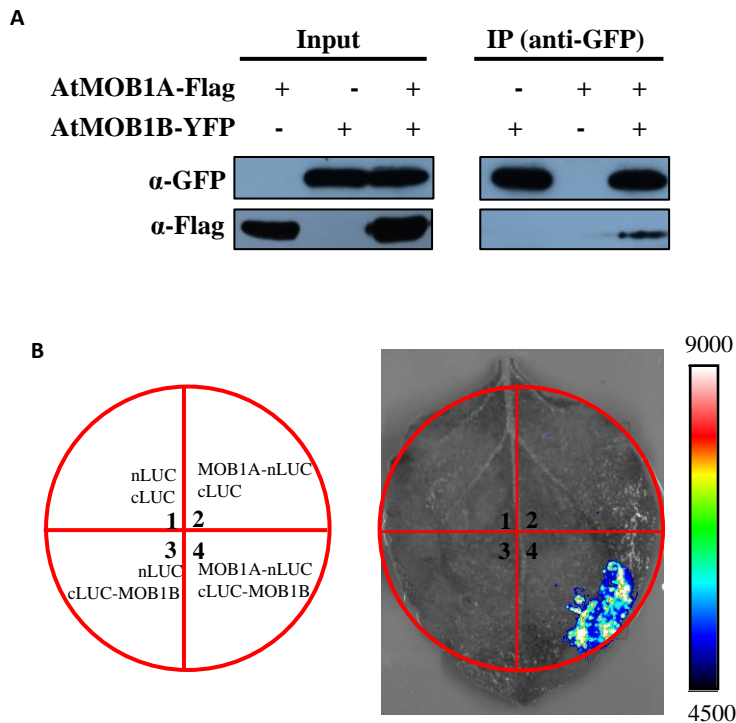


**Figure 3. Physical interaction between AtMOB1A and AtMOB1B proteins in vivo.**

(A) Co-IP assay of AtMOB1A and AtMOB1B. AtMOB1B-GFP was immuno-precipitated by using anti-GFP agarose beads, followed by immunoblot with anti-Flag antibody, and AtMOB1A-Flag was detected. (B) LCI assays showing the interaction between MOB1A and MOB1B in *N. benthamiana* leaf cells. The left panel shows the combinations of agrobacteria containing the indicated plasmids used to co-infiltrate into different leaf regions of the right panel. Empty cLUC and nLUC vectors were used as negative controls. The experiments were carried out with three independent biological repeats.

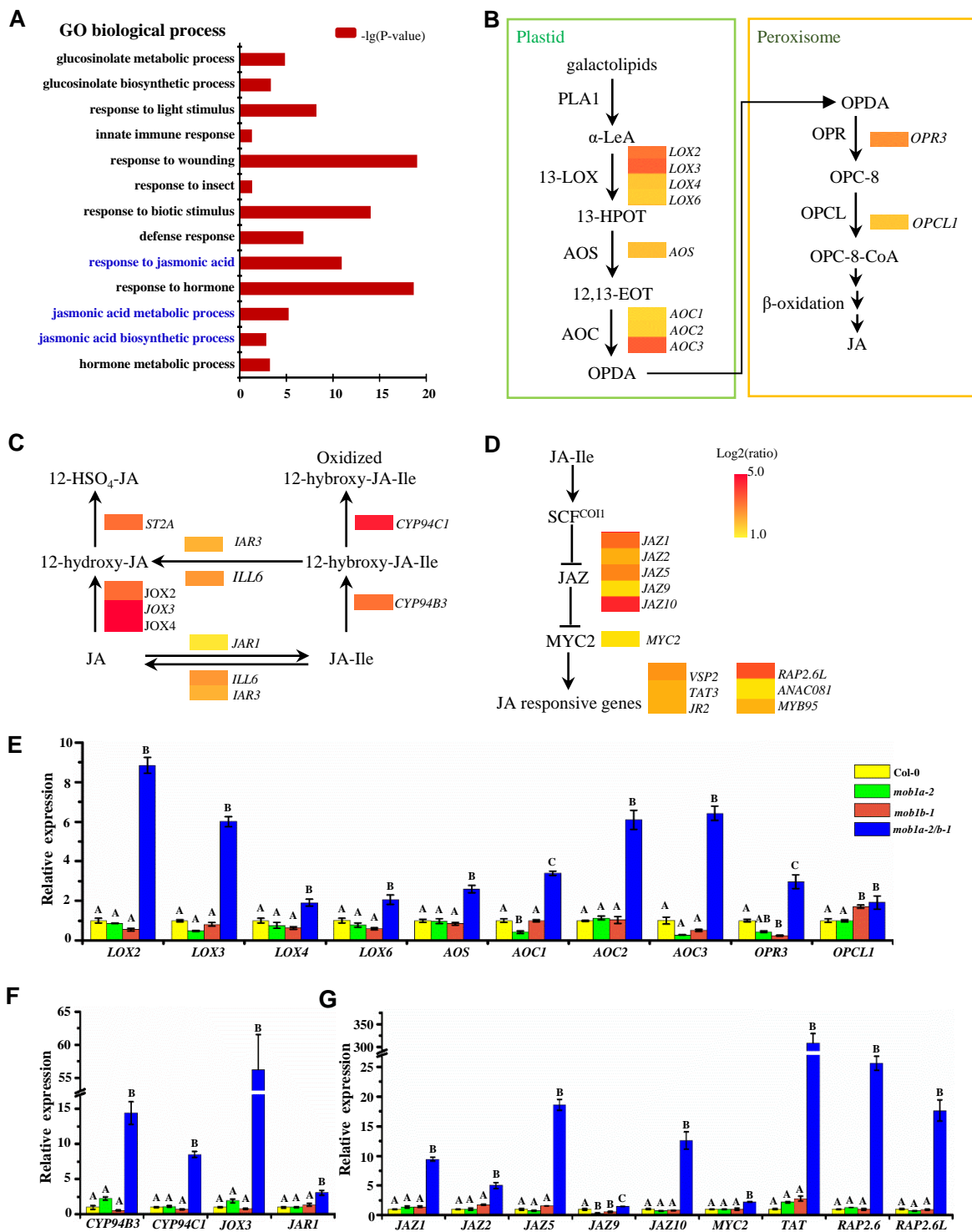


**Figure 4. Expression of genes involved in JA biosynthesis, metabolism, and signaling are altered in the *mob1a-2/b-1* double mutant.**

(A) Functional assignment of the DEGs by GO enrichment analysis. Bars represent  $-\lg(P\text{-value})$  and the P values were adjusted by the Bonferroni approach. (B-D) The DEGs in jasmonic acid biosynthesis (B), metabolic processes of JA and JA-Ile (C), and JA signaling pathway and response to JA (D). The Heatmap indicates the ratio being up-regulated. Scale colors represent  $\log_2(\text{ratio})$ .  $\alpha$ -LeA,  $\alpha$ -linolenic acid; 13-HPOT, 13-hydroperoxylinolenic acid; 12,13-EOT, 12,13-epoxyoctadecatrienoic acid; OPDA, 12-oxophytodienoic acid; OPC-8, 3-oxo-2-(2-pentenyl)-cyclopentane-1-octanoic acid; PLA1, phospholipase A1; 13-LOX, 13-lipoxygenase; AOS, allene oxide synthase; AOC, allene oxide cyclase; OPR, OPDA reductase; OPCL, OPC-8-CoA ligase; ST2A, 12-OH-JA sulfotransferase; JOX, jasmonic acid oxidase; JAR1, jasmonoyl isoleucine syntase; ILL6 and IAR3, IAA-amino acid hydrolase; CYP94C1; 12-OH-JA-Ile carboxylase; JAZ, jasmonate-zim-domain protein; MYC2, bHLH zip transcription factor; VSP2, vegetative storage protein 2; TAT3, tyrosine aminotransferase 3; JR2, jasmonic acid responsive 2; RAP2.6L, ERF/AP2 transcription factor; ANAC081, Arabidopsis NAC domain containing protein 81. (E-G) Relative expression of the DEGs in JA biosynthesis (E), metabolism (F), and signaling (G) in Col-0, *mob1a-2*, *mob1b-1*, and *mob1a-2/b-1*. 10-d-old seedlings were collected for RNA-Seq on 2019/7/17. The expression levels of the indicated genes in Col-0 were set to 1. Error bars represent the SD of three biological repeats. Different letters indicate significant difference at  $P < 0.001$  (one-way ANOVA, Tukey post test).

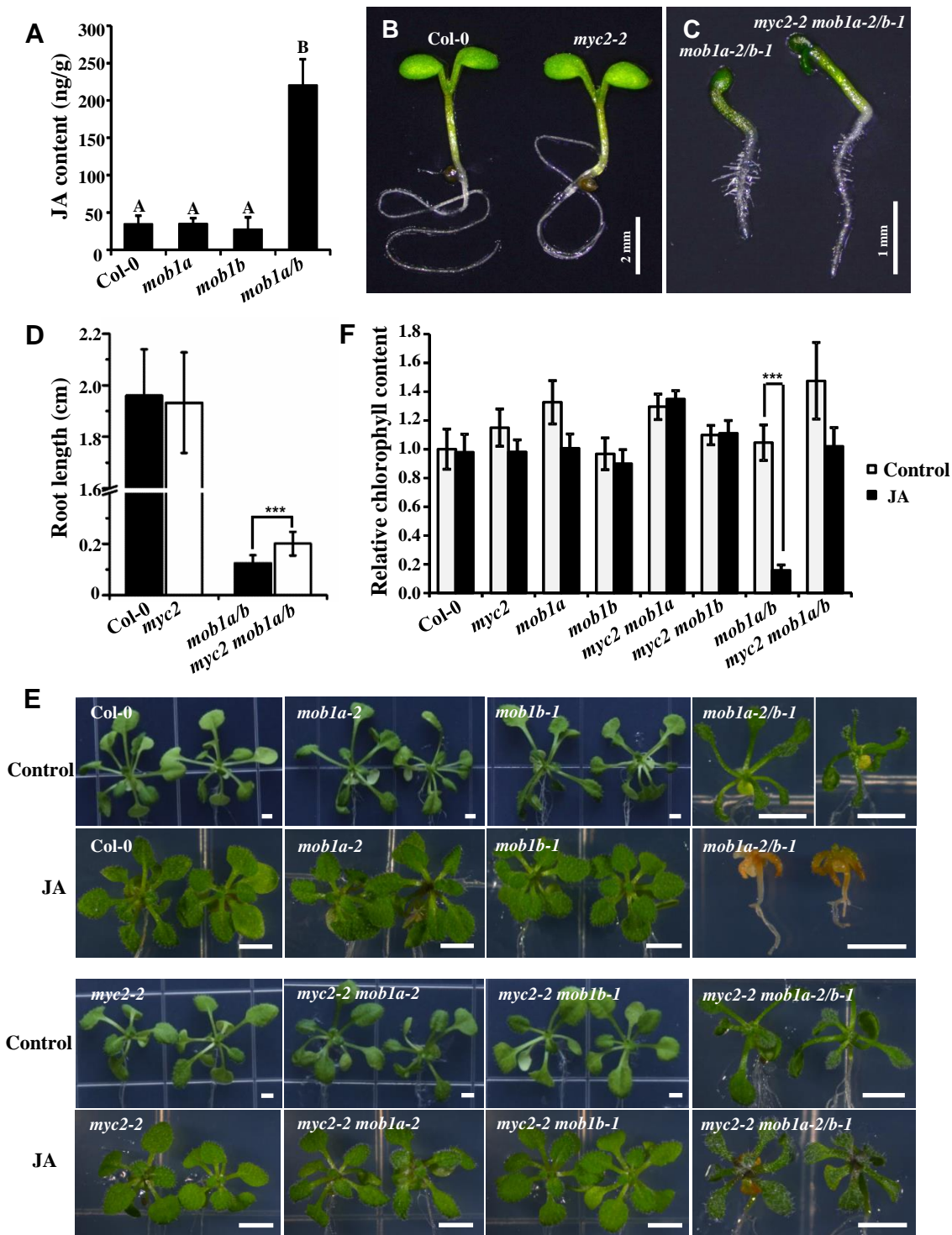


**Figure 5. AtMOB1A and AtMOB1B negatively regulate JA accumulation.** (A) Measurement of the JA contents in seedlings of Col-0, *mob1a-2*, *mob1b-1*, and *mob1a-2/b-1* mutants by using GC-MS. Seedlings were grown on 1/2 MS medium for 14 d after germination. Data represent means  $\pm$  SD of three independent biological repeats. Different letters represent statistical significance at the  $P < 0.001$  level (one-way ANOVA, LSD test). (B-C) 6-d-old seedlings of Col-0, *myc2-2*, *mob1a-2/b-1*, and *myc2-2 mob1a-2/b-1* mutants. Seedlings were grown on 1/2 MS medium for 6 d after germination. Scale bars: 2 mm (B), 1 mm (C). (D) Measurement of root length of Col-0, *myc2-2*, *mob1a-2/b-1*, and *myc2-2 mob1a-2/b-1* mutants. Data represent means  $\pm$  SD ( $n \geq 20$ ) with significant differences determined by Student's *t*-test. \*\*\* $P < 0.001$  compared to *mob1a-2/b-1*. (E) *mob1a-2/b-1* mutants were hypersensitive to exogenous JA treatment. 5-d-old seedlings grown on 1/2 MS plates were transferred to the 1/2 MS plates without (Control, upper panels) or with (JA, lower panels) 100  $\mu$ M Me-JA and grown for 2 weeks. Scale bars: 2 mm. (F) Measurement of chlorophyll contents. The chlorophyll contents of indicated mutants are relative to that in Col-0, which was set to 1.0. Data represent means  $\pm$  SD ( $n = 15$ ). Student's *t*-test. \*\*\* $P < 0.001$  compared to control.

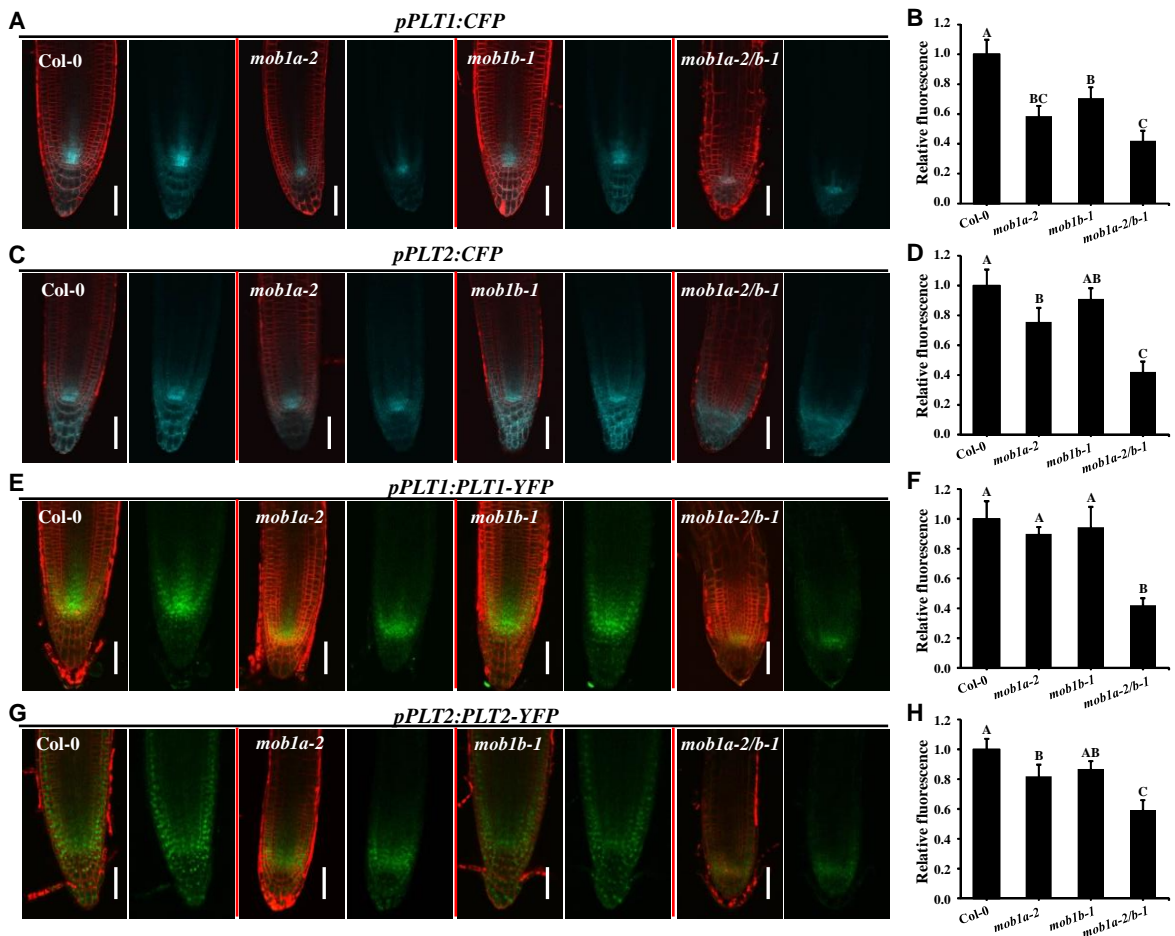


**Figure 6. Expression levels of *PLT1* and *PLT2* are reduced in *mob1a-2/b-1*.**

(A, C, E, G) Representative expression of *PLT1:CFP* (A), *PLT2:CFP* (C), *PLT1:PLT1-YFP* (E), and *PLT2:PLT2-YFP* (G) in the root tips of 6-d-old Col-0, *mob1a-2*, *mob1b-1*, and *mob1a-2/b-1* mutant seedlings. Scale bars: 50  $\mu$ m. (B, D, F, H) Quantification of CFP (A, C) and YFP (E, G) fluorescence, respectively. The fluorescence strength of Col-0 was set to 1. Data represent means  $\pm$  SD (n = 15). Different letters represent statistical significance at the P < 0.001 level (one-way ANOVA, LSD test).

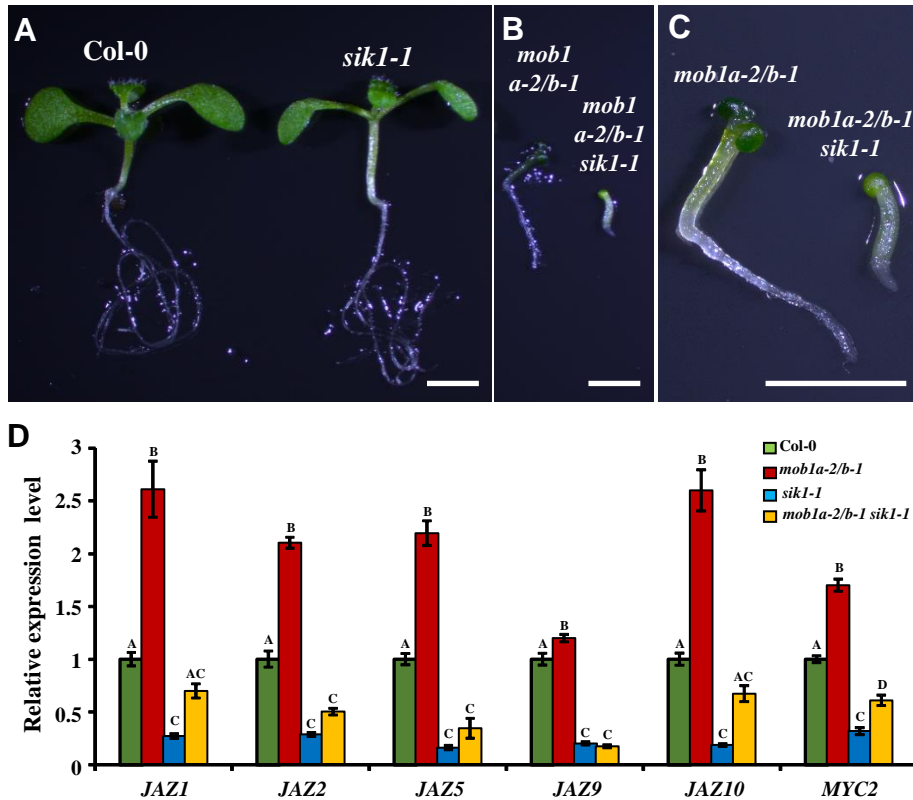


**Figure 7. Genetic interaction between *MOBIA/B* and *SIK1*.**

(A-B) 12-d-old seedlings of Col-0, *sik1-1*, *mob1a-2/b-1* and *mob1a-2/b-1 sik1-1* mutants. (C) Close-up of seedlings in (B). Note the triple mutant was smaller than the double mutant. Scale bars: 2 mm (A-C). (D) Relative expression of JA signaling-related genes in 12-d-old seedlings of Col-0, *mob1a-2/b-1*, *sik1-1* and *mob1a-2/b-1 sik1-1*. *ACTIN2* was used as an internal control. The expression levels of the indicated genes in Col-0 were set to 1. Different letters indicate significant difference at  $P < 0.001$  ( $n = 3$ , one-way ANOVA, Tukey post test).

## Parsed Citations

**Aida M, Beis D, Heidstra R, Willemsen V, Bliou I, Galinha C, Nussaume L, Noh YS, Amasino R, Scheres B (2004) The PLETHORA genes mediate patterning of the Arabidopsis root stem cell niche. Cell 119: 109-120**

Pubmed: [Author and Title](#)

Google Scholar: [Author Only Title Only Author and Title](#)

**Chen H, Zou Y, Shang Y, Lin H, Wang Y, Cai R, Tang X, Zhou JM (2008) Firefly luciferase complementation imaging assay for protein-protein interactions in plants. Plant Physiol 146: 368-376**

Pubmed: [Author and Title](#)

Google Scholar: [Author Only Title Only Author and Title](#)

**Chen Q, Sun J, Zhai Q, Zhou W, Qi L, Xu L, Wang B, Chen R, Jiang H, Qi J, Li X, Palme K, Li C (2011) The basic helix-loop-helix transcription factor MYC2 directly represses PLETHORA expression during jasmonate-mediated modulation of the root stem cell niche in Arabidopsis. Plant Cell 23: 3335-3352**

Pubmed: [Author and Title](#)

Google Scholar: [Author Only Title Only Author and Title](#)

**Chow A, Hao Y, Yang X (2010) Molecular characterization of human homologs of yeast MOB1. Int J Cancer 126: 2079-2089**

Pubmed: [Author and Title](#)

Google Scholar: [Author Only Title Only Author and Title](#)

**Citterio S, Piatti S, Albertini E, Aina R, Varotto S, Barcaccia G (2006) Alfalfa Mob1-like proteins are involved in cell proliferation and are localized in the cell division plane during cytokinesis. Exp Cell Res 312: 1050-1064**

Pubmed: [Author and Title](#)

Google Scholar: [Author Only Title Only Author and Title](#)

**Colon-Carmona A, You R, Haimovitch-Gal T, Doerner P (1999) Technical advance: spatio-temporal analysis of mitotic activity with a labile cyclin-GUS fusion protein. Plant J 20: 503-508**

Pubmed: [Author and Title](#)

Google Scholar: [Author Only Title Only Author and Title](#)

**Cui X, Guo Z, Song L, Wang Y, Cheng Y (2016) NCP1/AtMOB1A Plays Key Roles in Auxin-Mediated Arabidopsis Development. PLoS Genet 12: e1005923**

Pubmed: [Author and Title](#)

Google Scholar: [Author Only Title Only Author and Title](#)

**Galinha C, Hofhuis H, Luijten M, Willemsen V, Bliou I, Heidstra R, Scheres B (2007) PLETHORA proteins as dose-dependent master regulators of Arabidopsis root development. Nature 449: 1053-1057**

Pubmed: [Author and Title](#)

Google Scholar: [Author Only Title Only Author and Title](#)

**Galla G, Zenoni S, Marconi G, Marino G, Botton A, Pinosa F, Citterio S, Ruperti B, Palme K, Albertini E, Pezzotti M, Mau M, Sharbel TF, De Storme N, Geelen D, Barcaccia G (2011) Sporophytic and gametophytic functions of the cell cycle-associated Mob1 gene in Arabidopsis thaliana L. Gene 484: 1-12**

Pubmed: [Author and Title](#)

Google Scholar: [Author Only Title Only Author and Title](#)

**Gao X, Chen J, Dai X, Zhang D, Zhao Y (2016) An Effective Strategy for Reliably Isolating Heritable and Cas9-Free Arabidopsis Mutants Generated by CRISPR/Cas9-Mediated Genome Editing. Plant Physiol 171: 1794-1800**

Pubmed: [Author and Title](#)

Google Scholar: [Author Only Title Only Author and Title](#)

**Goto H, Nishio M, To Y, Oishi T, Miyachi Y, Maehama T, Nishina H, Akiyama H, Mak TW, Makii Y, Saito T, Yasoda A, Tsumaki N, Suzuki A (2018) Loss of Mob1a/b in mice results in chondrodysplasia due to YAP1/TAZ-TEAD-dependent repression of SOX9. Development 145**

Pubmed: [Author and Title](#)

Google Scholar: [Author Only Title Only Author and Title](#)

**Hansen CG, Moroishi T, Guan KL (2015) YAP and TAZ: a nexus for Hippo signaling and beyond. Trends Cell Biol 25: 499-513**

Pubmed: [Author and Title](#)

Google Scholar: [Author Only Title Only Author and Title](#)

**Harvey KF, Zhang X, Thomas DM (2013) The Hippo pathway and human cancer. Nat Rev Cancer 13: 246-257**

Pubmed: [Author and Title](#)

Google Scholar: [Author Only Title Only Author and Title](#)

**He Y, Fukushige H, Hildebrand DF, Gan S (2002) Evidence supporting a role of jasmonic acid in Arabidopsis leaf senescence. Plant Physiol 128: 876-884**

Pubmed: [Author and Title](#)

Google Scholar: [Author Only Title Only Author and Title](#)

**Huang H, Liu B, Liu L, Song S (2017) Jasmonate action in plant growth and development. J Exp Bot 68: 1349-1359**

Pubmed: [Author and Title](#)

Google Scholar: [Author Only Title Only Author and Title](#)

Lai ZC, Wei X, Shimizu T, Ramos E, Rohrbach M, Nikolaidis N, Ho LL, Li Y (2005) Control of cell proliferation and apoptosis by mob as tumor suppressor, *mats*. *Cell* 120: 675-685

Pubmed: [Author and Title](#)

Google Scholar: [Author Only](#) [Title Only](#) [Author and Title](#)

Li B, Dewey CN (2011) RSEM: accurate transcript quantification from RNA-Seq data with or without a reference genome. *BMC Bioinformatics* 12: 323

Pubmed: [Author and Title](#)

Google Scholar: [Author Only](#) [Title Only](#) [Author and Title](#)

Lorenzo O, Chico JM, Sanchez-Serrano JJ, Solano R (2004) JASMONATE-INSENSITIVE1 encodes a MYC transcription factor essential to discriminate between different jasmonate-regulated defense responses in Arabidopsis. *Plant Cell* 16: 1938-1950

Pubmed: [Author and Title](#)

Google Scholar: [Author Only](#) [Title Only](#) [Author and Title](#)

Luca FC, Winey M (1998) MOB1, an essential yeast gene required for completion of mitosis and maintenance of ploidy. *Mol Biol Cell* 9: 29-46

Pubmed: [Author and Title](#)

Google Scholar: [Author Only](#) [Title Only](#) [Author and Title](#)

Nishio M, Hamada K, Kawahara K, Sasaki M, Noguchi F, Chiba S, Mizuno K, Suzuki SO, Dong Y, Tokuda M, Morikawa T, Hikasa H, Eggenschwiler J, Yabuta N, Nojima H, Nakagawa K, Hata Y, Nishina H, Mimori K, Mori M, Sasaki T, Mak TW, Nakano T, Itami S, Suzuki A (2012) Cancer susceptibility and embryonic lethality in Mob1a/1b double-mutant mice. *J Clin Invest* 122: 4505-4518

Pubmed: [Author and Title](#)

Google Scholar: [Author Only](#) [Title Only](#) [Author and Title](#)

Nishio M, Sugimachi K, Goto H, Wang J, Morikawa T, Miyachi Y, Takano Y, Hikasa H, Itoh T, Suzuki SO, Kurihara H, Aishima S, Leask A, Sasaki T, Nakano T, Nishina H, Nishikawa Y, Sekido Y, Nakao K, Shin-Ya K, Mimori K, Suzuki A (2016) Dysregulated YAP1/TAZ and TGF-beta signaling mediate hepatocarcinogenesis in Mob1a/1b-deficient mice. *Proc Natl Acad Sci U S A* 113: E71-80

Pubmed: [Author and Title](#)

Google Scholar: [Author Only](#) [Title Only](#) [Author and Title](#)

Pan D (2010) The hippo signaling pathway in development and cancer. *Dev Cell* 19: 491-505

Pubmed: [Author and Title](#)

Google Scholar: [Author Only](#) [Title Only](#) [Author and Title](#)

Pinosa F, Begheldo M, Pasternak T, Zermiani M, Paponov IA, Dovzhenko A, Barcaccia G, Ruperti B, Palme K (2013) The Arabidopsis thaliana Mob1A gene is required for organ growth and correct tissue patterning of the root tip. *Ann Bot* 112: 1803-1814

Pubmed: [Author and Title](#)

Google Scholar: [Author Only](#) [Title Only](#) [Author and Title](#)

Qi T, Wang J, Huang H, Liu B, Gao H, Liu Y, Song S, Xie D (2015) Regulation of Jasmonate-Induced Leaf Senescence by Antagonism between bHLH Subgroup IIIe and III d Factors in Arabidopsis. *Plant Cell* 27: 1634-1649

Pubmed: [Author and Title](#)

Google Scholar: [Author Only](#) [Title Only](#) [Author and Title](#)

Shan X, Wang J, Chua L, Jiang D, Peng W, Xie D (2011) The role of Arabidopsis Rubisco activase in jasmonate-induced leaf senescence. *Plant Physiol* 155: 751-764

Pubmed: [Author and Title](#)

Google Scholar: [Author Only](#) [Title Only](#) [Author and Title](#)

Titarenko E, Rojo E, Leon J, Sanchez-Serrano JJ (1997) Jasmonic acid-dependent and -independent signaling pathways control wound-induced gene activation in Arabidopsis thaliana. *Plant Physiol* 115: 817-826

Pubmed: [Author and Title](#)

Google Scholar: [Author Only](#) [Title Only](#) [Author and Title](#)

Vitolo N, Vezzi A, Galla G, Citterio S, Marino G, Ruperti B, Zermiani M, Albertini E, Valle G, Barcaccia G (2007) Characterization and evolution of the cell cycle-associated mob domain-containing proteins in eukaryotes. *Evol Bioinform Online* 3: 121-158

Pubmed: [Author and Title](#)

Google Scholar: [Author Only](#) [Title Only](#) [Author and Title](#)

Wang W, Li X, Huang J, Feng L, Dolinta KG, Chen J (2014) Defining the protein-protein interaction network of the human hippo pathway. *Mol Cell Proteomics* 13: 119-131

Pubmed: [Author and Title](#)

Google Scholar: [Author Only](#) [Title Only](#) [Author and Title](#)

Wasternack C, Song S (2017) Jasmonates: biosynthesis, metabolism, and signaling by proteins activating and repressing transcription. *J Exp Bot* 68: 1303-1321

Pubmed: [Author and Title](#)

Google Scholar: [Author Only](#) [Title Only](#) [Author and Title](#)

Xiao S, Dai L, Liu F, Wang Z, Peng W, Xie D (2004) COS1: an Arabidopsis coronatine insensitive1 suppressor essential for regulation of jasmonate-mediated plant defense and senescence. *Plant Cell* 16: 1132-1142

Pubmed: [Author and Title](#)

Downloaded from on December 20, 2019 - Published by www.plantphysiol.org  
Copyright © 2019 American Society of Plant Biologists. All rights reserved.

Google Scholar: [Author Only](#) [Title Only](#) [Author and Title](#)

**Xiong J, Cui X, Yuan X, Yu X, Sun J, Gong Q (2016) The Hippo/STE20 homolog SIK1 interacts with MOB1 to regulate cell proliferation and cell expansion in Arabidopsis. J Exp Bot 67: 1461-1475**

Pubmed: [Author and Title](#)

Google Scholar: [Author Only](#) [Title Only](#) [Author and Title](#)

**Zeng W, Dai X, Sun J, Hou Y, Ma X, Cao X, Zhao Y, Cheng Y (2018) Modulation of auxin signaling and development by polyadenylation machinery. Plant Physiol**

Pubmed: [Author and Title](#)

Google Scholar: [Author Only](#) [Title Only](#) [Author and Title](#)

**Zhang M, Chiang YH, Toruno TY, Lee D, Ma M, Liang X, Lal NK, Lemos M, Lu YJ, Ma S, Liu J, Day B, Dinesh-Kumar SP, Dehesh K, Dou D, Zhou JM, Coaker G (2018) The MAP4 Kinase SIK1 Ensures Robust Extracellular ROS Burst and Antibacterial Immunity in Plants. Cell Host Microbe 24: 379-391 e375**

Pubmed: [Author and Title](#)

Google Scholar: [Author Only](#) [Title Only](#) [Author and Title](#)